Transient Elasticity and Polymeric Fluids: Small Amplitude Deformations

Oliver Müller[1], Mario Liu[1], Harald Pleiner[2] and Helmut R. Brand[3,2]
[1] *Institut für Theoretische Physik, Universität Tübingen, 72076 Tübingen, Germany.*
[2] *Max Planck Institute for Polymer Research, 55021 Mainz, Germany.*
[3] *Department of Physics, University of Bayreuth, 95440 Bayreuth, Germany.*
(Dated: February 1, 2016)

Transient Elasticity (TE) is a concept useful for a systematic generalization of viscoelasticity. Due to its thermodynamic consistency, it naturally leads to a simple description of non-Newtonian effects displayed by polymeric fluids, granular media and other soft-matters. We employ a continuum-mechanical theory that is derived from TE and tailored to polymeric fluids, showing how it captures a surprisingly large number of phenomena in shear and elongational flows, including stationary, oscillatory and transient ones, also the flow down an inclined channel. Even the Weissenberg effect is well accounted for. This theory is applicable for small as well as large amplitude deformations. We concentrate on the former in the present paper, leaving the latter to a companion paper.

PACS numbers: 47.50.-d, 05.70.Ln, 83.50.-v, 83.10.-y

I. INTRODUCTION AND MOTIVATION

The hydrodynamic method is a powerful and top-down approach to describe the continuum-mechanical, macroscopic behavior of any condensed systems. Starting from the basic physics of the system (rather than a collection of characteristic experiments), one can use it to derive the appropriate continuum-mechanical, or better: hydrodynamic, theory. It is done by considering energy and momentum conservation simultaneously, combining both in a thermodynamically consistent way.

This approach has been applied to many systems, including superfluid Helium [1, 2] and nematic liquid crystals [3, 4]. The hydrodynamic theories are so accurate and encompassing that both systems – in spite of their considerable complexities – are accepted as well understood. Hereby, the basic physics for the superfluids is spontaneously broken gauge symmetry, for liquid crystals broken rotational ones; and the associated state variables are, respectively, the superfluid velocity and director. Given these, the structure of the hydrodynamic theory can be uniquely determined, including especially the explicit form of the stress tensor σ_{ij}.

For a host of complex fluids and soft materials, such as polymers, colloidal suspensions and granular matter, the circumstances are less clarified. Lacking a similarly clear idea of their basic physics, the prevailing macroscopic understanding is based on a collection of experimental observations. Very often, the rheological behavior is characterized as *non-Newtonian*, stressing the distance to the *simple Newtonian* ones. Typical non-Newtonian effects are linear visco-elasticity, shear thinning, elongational hardening, rod-climbing (Weissenberg effect), yield stress, viscoplasticity, and thixotropy. To account for them, there are many textbook models, including Maxwell, Jeffrey, Oldroyd, Giesekus, Leonov and the intricate KBKZ [5–8]. All are designed bottom-up, with these effects in mind, by skillfully combining fluid dynamic insights, elasticity theory, and the frame-indifference principle. Starting from momentum conservation, $\dot{g}_i + \nabla_j \sigma_{ij} = 0$, they provide a *constitutive relation* that specifies the time derivative of $\sigma_{k\ell}$ as a function of the rate of stretching $A_{k\ell} \equiv \frac{1}{2}(\nabla_k v_\ell + \nabla_\ell v_k)$ and $\sigma_{k\ell}$ itself. Though no model is encompassing, or generally accepted as authoritative, the more sophisticated ones are well capable of accounting for a number of these experiments.

In recent years, the approach of constitutive relations has been supplemented by sophisticated mesoscopic models of local and transient substructures, such as the tube model for polymer melts [9]. Consequently, rather more complicated equations have been employed that, on one hand, are better at reproducing even the slightest details of an experiment, but on the other, frequently require separate descriptions for each new experiment. For instance, the description of shear flow [10] is different from that of elongational ones [11], and branched polymers require a treatment distinct from linear ones [12].

Instead of tailoring yet another constitutive relation, we aim to identify the basic physics of polymeric fluids, searching for qualitative understanding rather than faithful rendition. This can be done only by starting from a proposition to derive the associated hydrodynamics and check its results against observations. Taking *transient elasticity* (TE) as the basic physics of polymeric fluids, we have derived the associated hydrodynamic theory [13–16], and are in the present paper working out its results.

The variable associated with TE is the *elastic strain* U_{ij} *– the part of the total strain that leads to reversible storage of elastic energy.* The rest of the strain does not store any energy, is plastic and irrelevant. To account for the non-permanency of elasticity, U_{ij} is taken as a relaxing variable. All this is in contrast to true elasticity, in which the total strain, completely elastic and non-relaxing, always leads to energy storage. As nonlinear terms are important, we take U_{ij} to be the Eulerian strain tensor that vanishes in the absence of any deformation.

Without energy input, a TE-system is elastic for time

spans much smaller than the relaxation time τ of U_{ij}, $t \ll \tau$. For $t \gg \tau$, $U_{ij} = 0$ is relaxed, there is no elastic stress, and the system is fluid. With input, such as under a steady shear flow, circumstances are more subtle. We note it is not at all obvious that by making viscoelasticity thermodynamically consistent will yield a model capable of accounting for characteristic polymeric effects: shear thinning, normal stress differences, and others. Yet applying the TE-hydrodynamics to varying flows, we find a surprisingly wide range of instances that display satisfactory agreement to experimental observations.

Any hydrodynamic theory has two parts, structure and coefficients. To set up the structure, one first defines a set of state variables associated to the postulated basic physics. It is crucial for this set to be complete. Only then is the hydrodynamic theory local in space and time, with gradient expansion rather than integral equations. And there are no hysteresis or history-dependence. We take the variables to be the elastic strain U_{ij}, in addition to the densities of mass and entropy: ρ, s. The total, conserved energy $\varepsilon^{\rm rf}$ in the rest frame is a function of them, $\varepsilon^{\rm rf} = \varepsilon^{\rm rf}(\rho, s, U_{ij})$. The conjugate variables are partial derivatives of $\varepsilon^{\rm rf}$, eg. $\psi_{ij} \equiv \partial\varepsilon^{\rm rf}/\partial U_{ij}$. ($\psi_{ij}$ is the elastic stress to linear order in U_{ij}. The complete expression is given in Eq.(4) below.) Without specifying $\varepsilon^{\rm rf}(\rho, s, U_{ij})$, all conjugate variables, especially ψ_{ij}, are formal, abstract quantities.

The dynamic equations for the state variables ρ, s, U_{ij} and for the momentum densities ρv_i define the fluxes, with the total stress tensor σ_{ij} given by the momentum flux. Ensuring energy, momentum and mass conservation, and the validity of the second law of thermodynamics, all fluxes may be uniquely determined, in terms of the state and conjugate variables. They hold irrespective what form $\varepsilon^{\rm rf}(\rho, s, U_{ij})$ has. The fluxes contain transport coefficients that are frequently taken as constant, but are generally functions of the state variables. A discussion of the hydrodynamic framework and the elastic strain is in [13–16] and a comparison to conventional approaches in [17]. The advantages of this method are (1) its explicit compliance with general principles including conservation laws, thermodynamics and symmetry requirements; and (2) its easy generalization to incorporate additional variables (such as the elastic strain).

To arrive at a concrete theory, one that may be tested against experiments, the energy $\varepsilon^{\rm rf}$ and the transport coefficients need to be specified. These are material-dependent properties that reflect, on the macroscopic level, the microscopic structures and properties. There is no systematic treatment, and we had to resort to a trial-and-error approach. The expressions given in Sec.II are found appropriate for standard polymeric fluids.

It is useful in this context to note the similarities between some soft matter systems. For instance, granular media are also characterized by TE and the elastic strain U_{ij}, although the elastic energy $\varepsilon^{\rm rf}$ is completely different [18–21]. (In addition, the granular temperature T_g is needed as a variable). Again, a wide range of experiments were shown well accounted for by its hydrodynamics [22]. Colloidal suspensions and yielding soft matter are prime candidates for a similar treatment in the future.

In Sec.II, a simplified version of the TE-hydrodynamics named *the polymeric hydrodynamics*, as derived and argued for in the Appendix, is presented. The energy and the transport coefficients are specified such that the equations are simple enough for an analytic or quasi-analytic treatment, rendering the physics underlying polymeric effects such as shear thinning, elongational hardening and rod climbing transparent. We employ it to study shear flows in Sec. III, and elongational ones in Sec. IV – both confined to small strains, leaving the case of large deformations to the companion paper (II).

II. THE POLYMERIC HYDRODYNAMICS

The TE-hydrodynamics, as given in Refs. [13–16], is general. It accounts not only for various flows, but also for sound propagation, temperature diffusion, and other hydrodynamic phenomena, many of less interest at the moment. Therefore, we take the liquid to be incompressible and isothermal, $T, \rho = \text{const}$, $A_{\ell\ell} = 0$. In addition, we have $U_{kk} = 0$ for linear elasticity. As this is insufficient for our purposes, we employ the general condition [7],

$$(1 - 2U_1)\,(1 - 2U_2)\,(1 - 2U_3) = 1, \tag{1}$$

with U_i the eigenvalues of U_{ij}. Its dynamic equation is

$$\begin{aligned} \dot{U}^0_{ij} + v_k\nabla_k U^0_{ij} + \left[U_{kj}\nabla_i v_k + U_{ik}\nabla_j v_k\right]^0 \\ = A^0_{ij} - U^0_{ij}/\tau, \qquad \tau > 0, \end{aligned} \tag{2}$$

where the superscript 0 denotes the traceless part. Clearly, viscoelasticity is codified by the term $-U^0_{ij}/\tau$. The conservation of momentum sports three stress terms:

$$\rho\,(\dot{v}_i + v_k\nabla_k v_i) + \nabla_i P + \nabla_j(\sigma^{\rm ela}_{ij} - \sigma^{\rm D}_{ij}) = 0, \tag{3}$$

$$\sigma^{\rm ela}_{ij} = -\psi_{ij} + \psi_{ki}U_{jk} + \psi_{kj}U_{ik}, \tag{4}$$

$$\sigma^{\rm D}_{ij} = 2\eta_\infty A^0_{ij}, \quad \eta_\infty > 0, \tag{5}$$

$$P = -\varepsilon^{\rm rf} + Ts + \mu\rho, \tag{6}$$

$$\psi_{ij} \equiv \frac{\partial\varepsilon^{\rm rf}}{\partial U_{ij}}, \quad T \equiv \frac{\partial\varepsilon^{\rm rf}}{\partial s}, \quad \mu \equiv \frac{\partial\varepsilon^{\rm rf}}{\partial\rho}. \tag{7}$$

Next, we specify $\varepsilon^{\rm rf}$ by expanding it in U_{ij}. The general form to fourth order and the associated elastic stress are

$$\begin{aligned} \varepsilon^{\rm rf} - \bar{\varepsilon} =& K_1 U_{ij}U_{ji}/2 + K_2 U_{ij}U_{jk}U_{ki}/3 \\ &+ K_3 U_{ij}U_{jk}U_{k\ell}U_{\ell i}/4, \qquad K_1 > 0. \end{aligned} \tag{8}$$

$$\begin{aligned} \sigma^{\rm ela}_{ij} =& -K_1 U_{ij} + (2K_1 - K_2)\,U_{ik}U_{kj} \\ &+ (2K_2 - K_3)\,U_{ik}U_{kl}U_{lj}, \end{aligned} \tag{9}$$

see the Appendix for derivation. We note it is the expansion that limits the validity of these expressions to small deformations. To guarantee the uniqueness of the

zero stress solution associated with eq.(8), we require the condition $K_2^2 < 2K_1K_3$. This condition will turn out to be consistent with all inequalities arising in the following. For the case of large deformations a detailed analysis is given in the companion paper (denoted by (II) throughout the present paper). We also note there are two transport coefficients, the relaxation time τ and the viscosity η_∞, and three elasticity coefficients, K_i, altogether five. The quantity $\bar{\varepsilon}$ contains the thermodynamic degrees of freedom of a usual liquid, which, however, do not play a role in the following.

III. SHEAR FLOWS

A. General considerations

We now consider the case of planar shear flows. We will apply the polymeric hydrodynamics to this geometry to see how well it captures the experimental observations. We first recall the geometry of simple shear from Fig. 1 and the general form of the velocity profile

$$\mathbf{v}\left(\mathbf{r},t\right) = v_x\left(y,t\right)\hat{\mathbf{x}}, \tag{10}$$

where $\hat{\mathbf{x}}$ is flow direction, $\hat{\mathbf{y}}$ the direction of the velocity changes and $\hat{\mathbf{z}}$ the neutral direction. The gradient $\nabla_y v_x$ is usually called shear rate and denoted by $\dot{\gamma}$ [28].

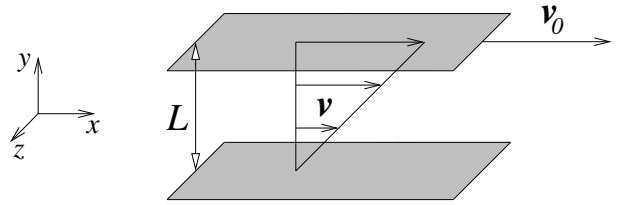

FIG. 1: *Planar shear flow between two parallel infinitely extended plates.*

For a start we must analyze the structure of the strain tensor U_{ij}. Considering a 2 D plane strain flow we have for U_{ij} and U_{ij}^0

$$\mathbf{U} = \begin{pmatrix} U_{xx} & U_{xy} \\ U_{yx} & U_{yy} \end{pmatrix} \tag{11}$$

$$\mathbf{U^0} = \begin{pmatrix} \frac{1}{2}(U_{xx}-U_{yy}) & U_{xy} \\ U_{yx} & \frac{1}{2}(U_{yy}-U_{xx}) \end{pmatrix}. \tag{12}$$

To get an intuitive picture of the deformations one can introduce the stretch coefficients λ_i [29]

$$\lambda_i = \frac{1}{\sqrt{1-2U_i}}\,, \quad i=1,2,3 \tag{13}$$

that describe the stretching along the principal axes relative to the unstrained geometry. Here, the eigenvalues of Eq. (11) are

$$U_{1,2} = \frac{1}{2}\left(U_{xx}+U_{yy} \mp U\right) \quad \text{and} \quad U_3 = 0 \tag{14}$$

with the abbreviation $U^2 = (U_{xx}-U_{yy})^2+4U_{xy}U_{yx}$. The orientation of the principal axes in the $x-y$ plane is given by the rotation angle ϕ, with

$$\tan\phi = \sqrt{\frac{U+U_{xx}-U_{yy}}{U-U_{xx}+U_{yy}}}. \tag{15}$$

It is useful to bring the dynamic equations for the strain tensor into a dimensionless form. U_{ij} itself is already dimensionless, time t and the shear rate $\dot{\gamma}$ will be given in units of the relaxation time

$$\xi \equiv \dot{\gamma}\tau \qquad d \equiv \frac{t}{\tau}. \tag{16}$$

The dimensionless shear rate ξ is called Weissenberg number in the rheology literature [7]. We will not use this terminology here, since the time scale τ arising here has a different origin than the one used historically in rheology.

Based on the translation symmetry in x- and z-direction we will also allow for the strain tensor only a y-dependence. We are now in a position to write down the three independent equations of motion for the strain components, Eqs. (2) and (1)in the form

$$\left(\dot{U}_{xx}-\dot{U}_{yy}\right)+\left(U_{xx}-U_{yy}\right) = 2\,\xi U_{xy} \tag{17}$$

$$\dot{U}_{xy}+U_{xy} = \frac{1}{2}\xi - \xi U_{xx} \tag{18}$$

$$U_{xx}+U_{yy} = 2\left(U_{xx}U_{yy}-U_{xy}^2\right), \tag{19}$$

where the dot denotes a partial derivative with respect to the dimensionless time d.

In spite of the numerous simplifications made, the resulting model for the motion of the upper plate without a well-determined velocity $v_0(t)$ is still difficult to solve. In addition to the three independent equations for U_{xx}, U_{yy} and U_{xy} given above, we must consider in addition a nontrivial diffusion equation for v_x given by Eq. (3), which also contains the components of the strain tensor. To address this complication we will assume as for Newtonian fluids that the velocity profile is linear. For Newtonian fluids this is a good approximation, when the distance between the plates is small and the viscosity is sufficiently high. This assumption therefore also appears to be a good ansatz for polymeric liquids. The shear rate is also independent of location, and from Eqs. (17) and (18) it follows automatically, that in this case also the strain tensor U_{ij} is spatially homogeneous. Thus Eq. (3) is reduced to the Navier-Stokes equation with η_∞ instead of η_0. This result suggests that the shear rate has the same structure as for a Newtonian fluid, namely $\dot{\gamma}(t) = v_0(t)/L$.

We are now ready to calculate the stress tensor in a polymeric fluid for a prescribed motion of the upper plate. To do this we proceed as follows: For a given $v_0(t)$ we assume that the shear rate is spatially homogeneous and has the same structure as a for a Newtonian fluid. Using Eqs. (17)-(19) and suitable initial conditions for

U_{xx}, U_{yy} and U_{xy} we can then calculate the strain tensor. From this result we determine the stress tensor σ_{ij} by Eqs. (5) and (9). In the following we will address the cases of planar stationary, relaxing and oscillatory shear flows as well as the onset of a planar shear flow. In addition we will analyze the Weissenberg (rod-climbing) effect and the flow down an inclined channel.

B. Stationary shear flow

The first and simplest case we will address is stationary shear flow. For this example we are particularly interested in the effects of shear thinning and the existence of normal stress differences. The upper plate is moving with constant velocity and the shear rate is therefore constant

$$\xi = \dot{\gamma}\tau = \text{const.} \tag{20}$$

In addition the strain tensor is time-independent, and the dynamic Eqs. (17)-(19) are reduced to

$$U_{xx} - U_{yy} = 2\,\xi U_{xy} \tag{21}$$

$$U_{xy} = \frac{1}{2}\,\xi - \xi\,U_{xx} \tag{22}$$

$$U_{xx} + U_{yy} = 2\,U_{xx}U_{yy} - 2\,U_{xy}^2. \tag{23}$$

This system of equations is straightforward to solve with the result

$$\mathbf{U} = \frac{1}{2}\begin{pmatrix} 1 - \frac{1}{\sqrt{1+\xi^2}} & \frac{\xi}{\sqrt{1+\xi^2}} \\ \frac{\xi}{\sqrt{1+\xi^2}} & 1 - \frac{1+2\xi^2}{\sqrt{1+\xi^2}} \end{pmatrix}, \tag{24}$$

where a second solution is ruled out because of the condition that the eigenvalues have to be smaller than 1/2.

As we have seen already from the equations of motion, the strain is in our simple approximation only a function of the dimensionless shear rate, its behavior is therefore universal. The non-vanishing components of U_{ij} are plotted in Fig. 2 as a function of ξ. We are plotting in Fig. 2 the components of the strain tensor for a large range of $\xi-$ values. While we focus in the present paper on small ξ- values, we will come back in a comparison to the behavior of larger $\xi-$ values in the companion paper (II).

Especially interesting for the purpose of the present paper is the case $|\xi| \ll 1$, since in that limit also the strain components are very small. Obviously, U_{xy} is linear in leading order, while the diagonal components are quadratic. The existence of diagonal components in a shear flow is a nonlinear effect, which is, as we will see shortly, essential for the description of the properties of polymeric fluids.

For a Newtonian fluid τ vanishes, therefore we can put $\xi = 0$ and see, that as expected the strain tensor vanishes. In the limit of an elastic solid we have $\tau \to \infty$, and we find from Eq. (24) an infinitely strong deformation U_{yy}. This result is also sensible, since in a solid maintaining a constant shear rate leads to an unbounded, all-the-time growing deformation. Of course, in praxis one cannot apply a constant shear to a solid, forever.

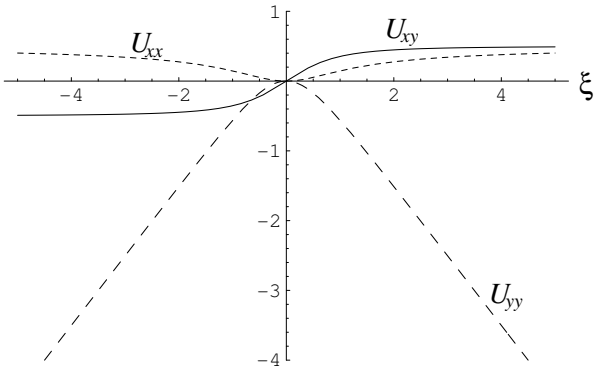

FIG. 2: *The components of the stationary strain tensor are plotted as a function of dimensionless shear rate. ξ.*

To visualize the deformation we calculate the stretch coefficients, λ_1, λ_2, along the principal strain axes

$$\lambda_{1,2} = \sqrt{\sqrt{1+\xi^2} \mp |\xi|} \tag{25}$$

and the rotation angle, ϕ, with respect to the laboratory system, $\tan\phi = \lambda_2/\lambda_1$.

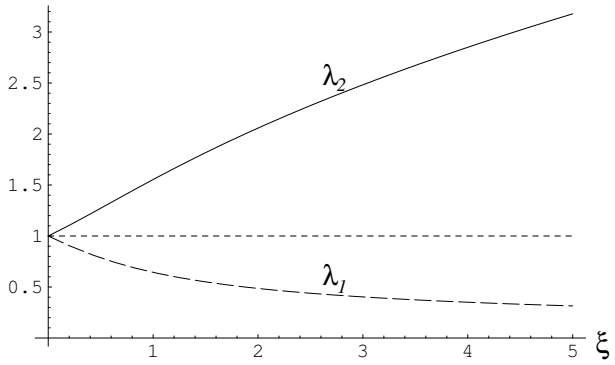

FIG. 3: *The stretch coefficients λ_1 and λ_2 are plotted as functions of the dimensionless shear rate ξ.*

For vanishing shear rate the system is undeformed and both stretch coefficients are one (Fig. 3). They are strictly monotonic functions of ξ, where for increasing ξ, λ_2 grows without bound and λ_1 converges to zero. From the incompressibility condition it follows that the product of the two stretch coefficients is unity independent of the shear rate. We wil come back to this figure showing also the large deformation behavior in the comparison given in the companion paper (II).

The orientation angle ϕ also reflects the behavior of λ_1 and λ_2 as a function of ξ. The strain axis turns away from the y-axis with growing shear rate and approaches asymptotically the x-axis, meaning the fluid is stretched parallel to the plates. For $\xi \to 0$ ϕ converges to 45°. This case, however, has no physical meaning, since it corresponds to the undeformed system.

Sample	η_0 in Pa s	$(\Psi_1)_0$ in Pa s^2	τ in s	K_1 in Pa
Polyethylene melt at $423K$ [30]	$5 \cdot 10^4$	$6 \cdot 10^6$	60	$2 \cdot 10^3$
2.0% Polyisobutylene in primol [5, 31]	10^3	$7 \cdot 10^4$	35	57
1.5% Polyacrylamide in a Water/Glycerol-Mixture [5, 31]	$3 \cdot 10^2$	$2 \cdot 10^4$	33	18
7% Aluminiumlaurate in a Decalin/m-Cresol-Mixture [5, 31]	90	$3 \cdot 10^2$	2	10^2
Linear Polydimethylsiloxane, LG1 [32]	$\sim 2 \cdot 10^4$	$\sim 2 \cdot 10^4$	~ 0.5	$\sim 10^5$
Linear Polydimethylsiloxane, LG2 [32]	$5 \cdot 10^5$	10^8	10^2	10^4

TABLE I: *Material parameters for various polymeric fluids.*

After we have characterized the behavior of the strain tensor, we now turn to the determination of the stress tensor for small values of the strain. The stress tensor for large deformations along with a consideration of the small deformation limit as a special case will be presented and discussed in (II). Since we have seen that the components U_{ij} are small when ξ is small, it is sensible to expand the strain tensor as well as the stress tensor into powers of ξ. Since we have expanded the elastic energy up to fourth order in the strains, the third order in ξ is the highest we can keep for the stress tensor without loosing contributions to the same order. We therefore expand the strain tensor Eq. (24) in powers of ξ and obtain, with Eqs. (5) and (9), for the non-vanishing components of the stress tensor, up to order ξ^3

$$\sigma_{xy} = -\frac{\eta_\infty}{\tau}\,\xi - \frac{1}{2}K_1\xi - \frac{1}{8}\,(2K_1 - 4K_2 + K_3)\,\xi^3 \quad (26)$$

$$\sigma_{xx} = \frac{1}{4}\,(K_1 - K_2)\,\xi^2 \quad (27)$$

$$\sigma_{yy} = \frac{1}{4}\,(5K_1 - K_2)\,\xi^2 \quad (28)$$

$$\sigma_{zz} = 0. \quad (29)$$

The stress tensor has the same symmetry properties as U_{ij}: while the diagonal elements are even functions of ξ and therefore independent of directions, the shear stress changes sign with the shear rate.

We are now in a position to calculate for small shear rates the three material functions that are commonly used to characterize a stationary shear flow [5]. We consider first the dynamic viscosity $\eta = -\sigma_{xy}/\dot{\gamma}$. It takes the form up to cubic order

$$\eta = \left(\eta_\infty + \frac{1}{2}K_1\tau\right) - \frac{1}{8}\,(-2K_1 + 4K_2 - K_3)\,\tau\xi^2. \quad (30)$$

Thus the shear viscosity is an even function of the shear rate. To obtain shear thinning, the quadratic contribution in ξ must be negative. This leads to a restriction for K_3

$$K_3 < 4K_2 - 2K_1. \quad (31)$$

It is obvious that we must introduce further conditions for the elastic constants to make sure that our model yields correctly shear thinning, since not all viscoelastic media are shear thinning. However, we will find out in the course of our discussions that a consistent picture for polymeric materials emerges. In the limit of a vanishing shear rate we obtain the so-called "zero-shear-rate viscosity" [5]

$$\eta_0 = \eta_\infty + \frac{1}{2}K_1\tau. \quad (32)$$

This quantity is not only determined by the viscosity constant η_∞, but also by the relaxation time and the elastic parameter K_1. This result follows already from linear elasticity while shear thinning is a truly nonlinear effect.

For the first and second normal stress difference, $\Psi_1 = -\left(\sigma_{xx} - \sigma_{yy}\right)/\dot{\gamma}^2$ and $\Psi_2 = -\left(\sigma_{yy} - \sigma_{zz}\right)/\dot{\gamma}^2$, we find, using eqs.(27) and (28)

$$\Psi_1 = K_1\tau^2 \quad \text{and} \quad \Psi_2 = -\frac{1}{4}\,(5K_1 - K_2)\,\tau^2. \quad (33)$$

We can thus obtain in the framework of our model the existence of normal stress differences. In the order considered here, the coefficients for these two quantities are constant; their dependence on shear rate arises only if one expands the elastic energy at least to fifth order in the strains. If one considers only linear contributions to the elastic stress, then Ψ_1 and Ψ_2 are identically zero; the existence of normal stress differences is thus uniquely a nonlinear elastic effect. As a rule Ψ_1 is positive and Ψ_2 is negative [5]. The first condition is always fulfilled, since $K_1 > 0$ by definition, while the second one requires additionally

$$K_2 < 5K_1. \quad (34)$$

The ratio of the normal stress coefficients is known to be typically about 0.1 [7]. In our model this requires $K_2 \sim 4.5K_1$ and K_2 is therefore obviously positive.

At the end of the present discussion we discuss the order of magnitude of the material parameters. Our goal is to determine from the observables Ψ_1 and η typical orders of magnitude for τ and K_1. We consider the limiting case of vanishing shear rates

$$\eta_0 \approx \frac{1}{2} K_1 \tau \quad \text{and} \quad (\Psi_1)_0 = K_1 \tau^2, \tag{35}$$

where we have assumed for simplicity that the elastic part of η is much larger than the dissipative one. This is motivated by the fact, that for shear thinning the shear viscosity can decrease by orders of magnitude. One will have to argue, however, that η_∞ is the limit of η for high shear rates; we will come back to this question when we discuss large deformations and high shear rates in the companion paper (II).

These relations can be inverted

$$\tau \approx \frac{(\Psi_1)_0}{2\eta_0} \quad \text{and} \quad K_1 \approx \frac{4\eta_0^2}{(\Psi_1)_0} \tag{36}$$

in order the calculate τ and K_1, if one knows the values of η_0 and $(\Psi_1)_0$ e.g. from extrapolations of measurements for $\eta(\dot\gamma)$ and $\Psi_1(\dot\gamma)$. In Table I the experimental values used are on the left and the calculated results on the right. Both, the relaxation time and the first elastic modulus for the various samples can vary by orders of magnitude. As a result, polymeric fluids are typically much more viscous than Newtonian liquids. For the two polydimethylsiloxane samples we can go further with the comparison. In [32] the empirical Carreau-Yasuda model is used to fit the measured curves $\eta(\dot\gamma)$ with τ_0 as one of the fit parameters. The results, $\tau_0 = 0.3\,\mathrm{s}$ for LG1 and 10^2s for LG2, agree well with our calculated values using Eq. (36).

The relaxation time τ has also consequences for the range of validity of the expansion in ξ – the smaller τ is, the larger the shear rates can be, for which the approximation is still applicable. This means, for example, that for very small relaxation times the two normal stress coefficients are still constants for higher shear rates. Similarly for the shear viscosity – the smaller the relaxation time, the flatter the shear thinning curve for small shear rates. This would suggest that, e.g., the shear viscosity for the aluminum laurate solution from Table I should decay much more slowly for small $\dot\gamma$ than for the polyisobutylene solution, which is clearly confirmed by Fig. 3.3-3 in [5].

To get a feeling for the values of the elastic constant K_1, we compare it with the elastic moduli of elastic solids. Rubber for example has a Young modulus of about $10^7 \ldots 10^8$Pa [33] and which is therefore two to three orders of magnitude higher than LG1, while the other samples tend to lie even well below this value. Because of the realistic estimate $K_2 \approx 4.5K_1$, K_2 is of the same order of magnitude as K_1. For K_3 such a statement is not possible, but we will give an estimate further below

Thus we have seen that the incorporation of nonlinear elastic properties yields the typical phenomena in a stationary shear flow. The price we had to pay were restrictions for the elastic constants K_2 and K_3. Next we will apply our model to time-dependent shear flows to see, how well other polymeric effects can be described by our ansatz and whether the restrictions for the elastic parameters can still be satisfied consistently.

C. Relaxing shear flow

In this section we will consider the case, when the upper plate for a stationary shear flow is stopped suddenly at a certain time. While in a viscous Newtonian fluid the liquid become quiescent rather fast and only the hydrostatic stress distribution is measured, one can observe in a polymeric fluid a slow non exponential relaxation of the stress [5]. To discuss this effect we assume for the shear rate the following time dependence

$$\dot\gamma(t) = \begin{cases} \dot\gamma_0 & \text{for } t < 0 \\ 0 & \text{for } t \geq 0. \end{cases} \tag{37}$$

This means that the upper plate comes to rest, and the velocity gradient vanishes, abruptly at time $t = 0$. In experiments it turns out that the time the fluid needs to come to rest is not zero, but still much smaller than the time scale for stress relaxation [34].

We begin again with the discussion of the strain tensor U_{ij}. For times $t < 0$ we have a stationary shear flow with the dimensionless shear rate $\xi_0 = \dot\gamma_0 \tau$ as discussed in the preceding section. For $t \geq 0$ the shear rate is identical to zero and the equations of motion for U_{ij}, Eqs. (17)-(19) read

$$\left(\dot U_{xx} - \dot U_{yy}\right) = -\left(U_{xx} - U_{yy}\right) \tag{38}$$

$$\dot U_{xy} = -U_{xy} \tag{39}$$

$$U_{xx} + U_{yy} = 2\left(U_{xx}U_{yy} - U_{xy}^2\right), \tag{40}$$

with the initial condition that for $t = 0$ the strain tensor has its stationary form Eq. (24). The dynamic equations immediately lead to an exponential relaxation of the difference of the diagonal components and the shear component

$$U_{xx} - U_{yy} = \frac{\xi_0^2\, e^{-d}}{\sqrt{1+\xi_0^2}} \tag{41}$$

$$U_{xy} = \frac{\xi_0\, e^{-d}}{2\sqrt{1+\xi_0^2}}, \tag{42}$$

with the characteristic time τ. Using these solutions the sum of the diagonal components follows from the incompressibility condition, Eq. (40), after some algebra

$$U_{xx} + U_{yy} = 1 - \sqrt{1 + \xi_0^2\, e^{-2d}}. \tag{43}$$

It shows a non-exponential decay to zero, due to the nonlinearities in the incompressibility condition. Although the relaxation is not exponential, τ sets the time scale. All other components are zero.

Also in this example the calculation of λ_1, λ_2 and ϕ is very useful. We find

$$\lambda_{1,2} = \left(\sqrt{1 + \xi_0^2\, e^{-2d}} \mp |\xi_0\, e^{-d}| \right)^{1/2} \tag{44}$$

and $\tan\phi = \lambda_2(d=0)/\lambda_1(d=0)$.

The results contain the surprising feature that the orientation of the system of principal axes does not depend on time during the relaxation, but maintains the orientation it had before the switch-off of the driving. The relaxation behavior of the stretch ratios also reveals an interesting property. For a fixed time d, λ_1 and λ_2 correspond to a stationary shear flow with the effective shear rate $\xi_{\rm eff} = \xi_0\, e^{-d}$. Since λ_1 and λ_2 are strictly monotonic functions of shear rate in the stationary case, it follows that both relax strictly monotonically to one, see also Fig. 4. An overshoot or an oscillatory behavior therefore does not occur within this model.

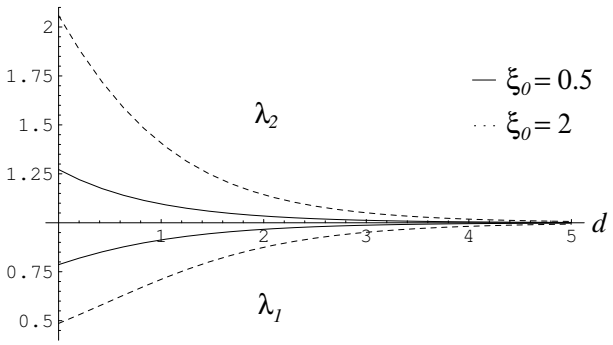

FIG. 4: *The stretch coefficients λ_1 and λ_2 as a function of time d for $\xi_0 = 0.5$ and $\xi_0 = 2$.*

For the calculation of the stress tensor we are again confined to the limit of small deformations. They are small not only for small stationary shear rates ξ_0 and arbitrary times d, but also for large times d and arbitrary shear rates ξ_0. We are mainly interested in the former case and expand U_{ij} into powers of ξ_0 up to third order

$$\mathbf{U} = \begin{pmatrix} \frac{1}{2}\left(1 - \frac{1}{2}e^{-d}\right) e^{-d}\,\xi_0^2 & \frac{1}{2}e^{-d}\,\xi_0 - \frac{1}{4}e^{-d}\,\xi_0^3 \\ \frac{1}{2}e^{-d}\,\xi_0 - \frac{1}{4}e^{-d}\,\xi_0^3 & -\frac{1}{2}\left(1 + \frac{1}{2}e^{-d}\right) e^{-d}\,\xi_0^2 \end{pmatrix}. \tag{45}$$

When calculating the stress tensor, we realize that its dissipative part $\sigma_{ij}^{\rm D}$ vanishes, since there is no flow for $d \geq 0$. We obtain for the non-vanishing components of σ_{ij} up to order ξ_0^3

$$\begin{aligned} \sigma_{xy} &= -\frac{1}{2}K_1 e^{-d}\,\xi_0(1 - \frac{1}{2}\xi_0^2) \\ &\quad + \frac{1}{8}\left(-4K_1 + 4K_2 - K_3\right) e^{-3d}\xi_0^3 \qquad (46) \\ \sigma_{xx} &= \left[-\frac{1}{2}K_1 e^{-d} + \frac{1}{4}\left(3K_1 - K_2\right) e^{-2d}\right] \xi_0^2 \qquad (47) \\ \sigma_{yy} &= \left[\frac{1}{2}K_1 e^{-d} + \frac{1}{4}\left(3K_1 - K_2\right) e^{-2d}\right] \xi_0^2. \qquad (48) \end{aligned}$$

For $d \to 0$, σ_{xx} and σ_{yy} go over to their stationary form, compare Eqs. (27)-(29), in contrast to σ_{xy} that does not have the contribution $-\eta_\infty\dot\gamma_0$ due to the lack of flow. We see that the stress tensor relaxes to zero in the form of a superposition of various relaxation processes with the characteristic times τ, $\tau/2$ and $\tau/3$; the weight of the respective contributions depends on the elastic constants and the shear rate.

For a relaxing shear flow material functions η^-, Ψ_1^- and Ψ_2^- are defined [5] analogously to η, Ψ_1 and Ψ_2 by using ξ_0 instead of ξ, since the latter is zero at the times, when they are considered.

From Eq. (46) it is obvious that $\eta^-\,(\xi_0, d) \equiv -\sigma_{xy}/\xi_0$ is monotonically relaxing in time. To compare the slope of η^- for various shear rates, we discuss the normalized function $\eta^-(\xi_0,d)/\eta^-(\xi_0,0)$, where $\eta^-(\xi_0,0)$ differs from η by the contribution η_∞. The slope of this normalized function should decrease for increasing values of ξ_0. To examine this question, we evaluate this function at $d = 0$ and find for the slope up to order ξ_0^3

$$\left.\frac{\partial}{\partial d}\,\frac{\eta^-(\xi_0,d)}{\eta^-(\xi_0,0)}\right|_{d=0} = -1 + \frac{1}{2}\left(-4 + 4\frac{K_2}{K_1} - \frac{K_3}{K_1}\right)\xi_0^2. \tag{49}$$

The correct physical behavior is obtained when the prefactor of the ξ_0^2 contribution is negative, which leads to a lower bound for K_3

$$K_3 > 4\left(K_2 - K_1\right). \tag{50}$$

If this inequality turns into an equality, the relaxation would be independent of ξ_0 (up to order ξ_0^3). This bound is not in contradiction to the upper bound, which was given by the inequality (31) and which followed from shear thinning. With the realistic estimate $K_2 \approx 4.5K_1$ this means that K_3 lies roughly between $14K_1$ and $16K_1$ and is thus obviously positive. For Fig. 5 we used the values $K_2 = 4.5K_1$ and $K_3 = 15K_1$.

It turns out that for small shear rates the curves for different ξ_0 are difficult to distinguish; this behavior is also known from experiment [34]. This can be used for an interesting comparison with experiments. The limiting curve, $\eta_0^-(d)$, of $\eta^-\,(\xi_0, d)$ for $\xi_0 \to 0$ serves as a (rather accurate) upper bound for all small-shear rate relaxation measurements. Its value, $\eta_0^-(d) = (1/2)K_1\tau\exp(-d)$, which already follows from linear elasticity theory, features τ as the relevant relaxation time scale. In Ref. [34]

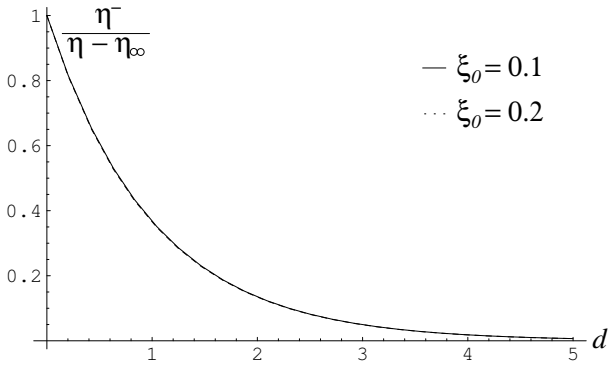

FIG. 5: *The material function η^- relative to the stationary value $\eta-\eta_\infty$ as a function of dimensionless time d for $\xi_0 = 0.1$ and $\xi_0 = 0.2$. We have used $K_2 = 4.5K_1$ and $K_3 = 15K_1$.*

sample	$\tau_{\rm exp}$ in s	τ in s
2.0% polyisobutylene in primol [34]	145	35
1.5% polyacrylamide in a water/glycerol- mixture [34]	104	33
7% Aluminiumlaurate in a Decaline/m-Cresol- mixture [34]	2.1	2

TABLE II: *Comparison of the various relaxation time scales $\tau_{\rm exp}$ and τ.*

the measured relaxation curves of η^- are compared with various models and this way characteristic time scales τ_{exp} are extracted. In Table II we compare these values with our calculated values of τ from Table I for those materials that were used in both, the stationary [31] and the relaxational measurements [34]. While for the aluminium soap solution the agreement of the time scales is very good, we find for the other samples a deviation by a factor of three to four. Since the time scales have a completely different origin, this deviation is to be expected, but we see nevertheless that the order of magnitude of both scales agrees.

The material functions $\Psi_1^- = -(\sigma_{xx}-\sigma_{yy})/\xi_0^2$ and $\Psi_2^- = -(\sigma_{yy}-\sigma_{zz})/\xi_0^2$ are (up to order ξ_0^2)

$$\Psi_1^-(\xi_0,d) = K_1\tau^2 e^{-d} \quad (51)$$

$$\Psi_2^-(\xi_0,d) = -\frac{1}{2}K_1\tau^2 e^{-d} + \frac{1}{4}(K_2-3K_1)\tau^2 e^{-2d}. \quad (52)$$

In the order considered these quantities do not depend on the stationary shear rate ξ_0 and Ψ_1^- relaxes purely exponentially. Comparing the relaxation behavior of Ψ_1^- and η^-, one finds experimentally, that

$$\frac{\Psi_1^-(\xi_0,d)}{\Psi_1^-(\xi_0,0)} > \frac{\eta^-(\xi_0,d)}{\eta^-(\xi_0,0)}. \quad (53)$$

In simple words this means that the first normal stress coefficient relaxes always more slowly than the viscosity, independently of ξ_0. Inserting our results into this inequality and expanding up to quadratic order in ξ_0, we obtain the relation

$$(4K_1 - 4K_2 + K_3)\left(e^{-2d}-1\right) < 0. \quad (54)$$

Since the second factor is always negative for $d > 0$, the resulting condition is identical with inequality (50). Therefore, if Eq. (50) is satisfied, the qualitative relaxation properties of Ψ_1^- and η^- are automatically given correctly.

Ψ_2^- is negative just like Ψ_2, when the condition (34), $K_2 < 5K_1$, is satisfied. In addition, the ratio Ψ_2^-/Ψ_2 shows an overshoot behavior at the beginning of the relaxation, when $K_2 > 4K_1$. In Fig. 6 this is the case, because of our estimate $K_2 \approx 4.5K_1$.

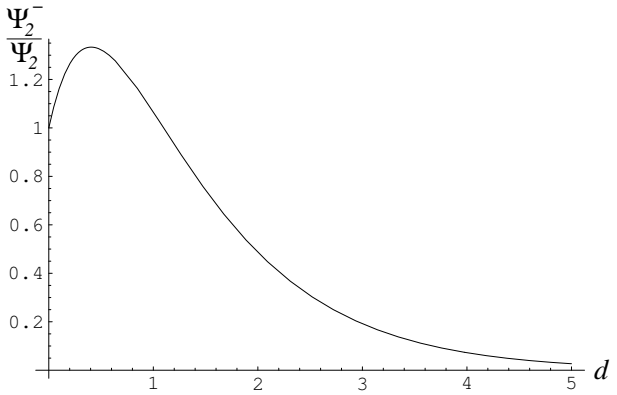

FIG. 6: *The material function Ψ_2^- relative to its stationary value Ψ_2 is plotted as a function of dimensionless time d with $K_2 = 4.5K_1$.*

To compare the solution for Ψ_2^- with experimental results is much more difficult than for Ψ_1^-, since the second normal stress difference is difficult to measure.

D. The onset of shear flow

In this section we discuss the complementary case compared to the last section, namely the onset of shear flow. In a fluid that is at rest initially, the upper plate starts moving at a specific time with constant velocity. In a fluid is at rest the upper plate suddenly starts moving with constant velocity. We expect that after some time a stationary shear flow results. While a Newtonian fluid reaches stationarity in the scheme presented on a negligible time scale, a polymeric fluid shows a convergence to a stationary behavior on the time scale τ. This convergence process is qualitatively different from the relaxation processes of the last section. For shear rates that are not too small, one finds for the components of the stress tensor a non-monotonic behavior in the form of an overshoot and afterwards an oscillatory convergence [5]. Since we are restricted to small shear rates here, we cannot give

in this paper a complete discussion of the overshoot, but we will get some interesting insights already. Therefore we start with the velocity profile

$$\dot{\gamma}(t) = \begin{cases} 0 & \text{for } t < 0 \\ \dot{\gamma}_0 & \text{for } t \geq 0 \end{cases}, \tag{55}$$

meaning that the upper plate starts moving with constant velocity, and the constant velocity gradient is established, abruptly at time $t = 0$. Of course, even this process takes a finite time, which we neglect however, compared to the time scale τ relevant for strain and stress convergence.

To determine the temporal behavior of the strain tensor for $t \geq 0$ we must solve Eqs. (17)-(19) with a spatially and temporally constant shear rate $\xi_0 = \dot{\gamma}_0 \tau$. As initial condition the deformations are zero at time $t = 0$. Due to the time dependence if the strain tensor, the equations have only a numerical solution. But since we are restricting ourselves in this paper to small deformations and thus to small shear rates, we can make an expansion

$$U_{xy}(\xi_0, d) = A(d)\,\xi_0 + C(d)\,\xi_0^3 + \mathcal{O}\left(\xi_0^5\right) \tag{56}$$
$$U_{xx}(\xi_0, d) = B_x(d)\,\xi_0^2 + \mathcal{O}\left(\xi_0^4\right) \tag{57}$$
$$U_{yy}(\xi_0, d) = B_y(d)\,\xi_0^2 + \mathcal{O}\left(\xi_0^4\right). \tag{58}$$

Writing down this ansatz we have already made use of symmetry properties of the components with respect to the shear rate. Inserting the ansatz and keeping track of the orders in ξ_0, we find

$$\dot{A} + A = \frac{1}{2} \tag{59}$$
$$B_x + B_y = -2A^2 \tag{60}$$
$$\left(\dot{B}_x - \dot{B}_y\right) + (B_x - B_y) = 2A \tag{61}$$
$$\dot{C} + C = -B_x, \tag{62}$$

with the boundary conditions $A(0) = B_x(0) = B_y(0) = C(0) = 0$. As solution we obtain with this method the non-vanishing strain components up to order ξ_0^3

$$U_{xy}(\xi_0, d) = \frac{1}{2}\left(1 - e^{-d}\right)\xi_0 + \frac{1}{4}\left[-1 + \left(2 + d^2\right)e^{-d} - e^{-2d}\right]\xi_0^3 \tag{63}$$
$$U_{xx}(\xi_0, d) = \frac{1}{4}\left(1 - 2de^{-d} - e^{-2d}\right)\xi_0^2 \tag{64}$$
$$U_{yy}(\xi_0, d) = \frac{1}{4}\left[-3 + 2\,(2 + d)\,e^{-d} - e^{-2d}\right]\xi_0^2. \tag{65}$$

We want to elucidate again the temporal behavior of the deformations by considering the stretch ratios $\lambda_{1,2}$, Eq. (13). The analytical expressions are rather involved and we only present a plot for two different dimensionless shear rates in Fig. 7

We notice two features: the strictly monotonic convergence towards the stationary state takes place on a time scale set by τ. For the small shear rates considered in this paper, an overshoot behavior is not visible, and the stretch ratios are almost symmetric with respect to 1 (for all times d).

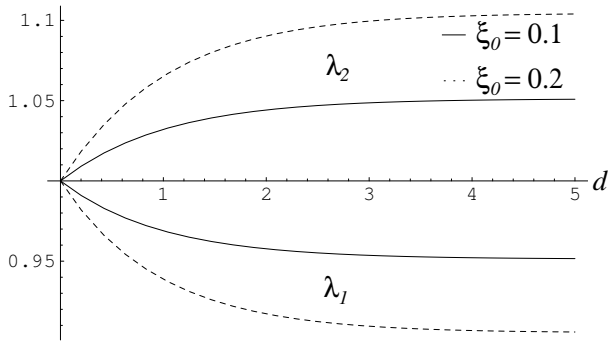

FIG. 7: *The stretch coefficients λ_1 and λ_2 are plotted as a function of time d for $\xi_0 = 0.1$ and $\xi_0 = 0.2$.*

Similarly, the temporal behavior of the orientation angle ϕ in Fig. 8 is monotonic In contrast to relaxing shear

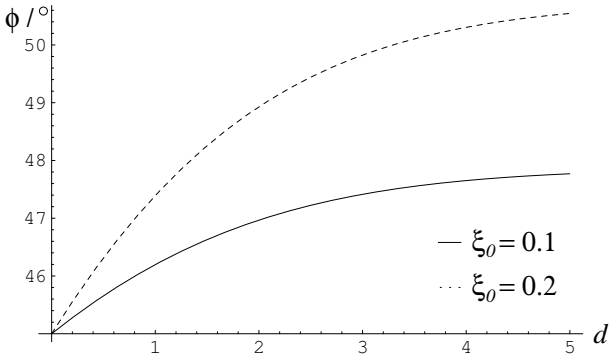

FIG. 8: *The orientation angle ϕ as a function of time τ for $\xi_0 = 0.1$ and $\xi_0 = 0.2$.*

flow ϕ is time-dependent in the present case. In the limit $d \to 0$ the angle reaches 45°, which was identified in section III B as the limiting case of vanishing shear rate. With increasing time it converges monotonically towards its stationary value.

For the calculation of the stress tensor σ_{ij} we proceed as usual. In contrast to the relaxing shear flow considered in the preceding section, here we do have a flow and the viscosity η_∞ enters as well. The material functions are defined such that for $d \to \infty$ they reach asymptotically the appropriate stationary values according to a shear rate ξ_0. in particular, for $\eta^+ = \sigma_{xy}/\xi_0$ we get

$$\eta^+(\xi_0, d) = \eta_\infty + \frac{1}{2}\left(1 - e^{-d}\right)K_1\tau + \frac{1}{8}\Gamma_2(d)\,\tau\,\xi_0^2, \tag{66}$$

with the abbreviation

$$\begin{aligned}\Gamma_2(d) &= (2K_1 - 4K_2 + K_3) \\ &+ \left(2\left[d^2-4\right]K_1 + 12K_2 - 3K_3\right)e^{-d} \\ &+ (10K_1 - 12K_2 + 3K_3)\,e^{-2d} \\ &+ (-4K_1 + 4K_2 - K_3)\,e^{-3d}.\end{aligned}$$

At time $d = 0$, $\eta^+ = \eta_\infty$ according to its definition, while for $d \to \infty$ it takes the stationary value $\eta(\xi_0)$ from Eq. (30). The behavior between these limits is visualized in Fig. 9. For the small values of ξ_0 considered here, the

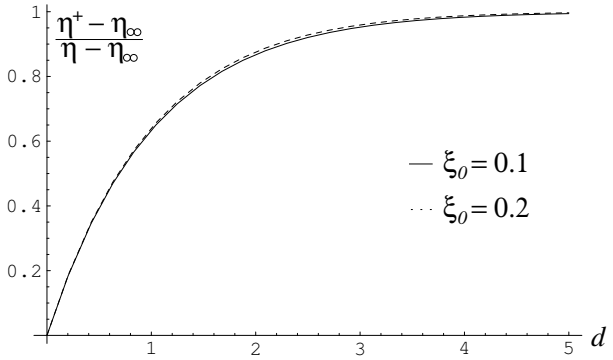

FIG. 9: *The material function η^+ relative to its stationary value η as a function of the dimensionless time d for $\xi_0 = 0.1$ and $\xi_0 = 0.2$. In addition, we have used $K_2 = 4.5K_1$ and $K_3 = 15K_1$.*

convergence towards the stationary value is monotonic and (slightly) faster for larger shear rates. This agrees with the observation for small shear rates [5]. The overshoot behavior occurring for higher shear rates cannot be obtained in the approximation considered here. Therefore, $\eta^+(0,d)$ is a lower bound for all small shear measurements. In addition, Ref. [34] refers to the relation $\eta^+(0,d)+\eta^-(0,d) = \eta(0)$, which is an exact result within linear elasticity description. It is trivially fulfilled by our expressions, but it is violated if extended to finite ξ_0 already in order ξ_0^2, as can be seen from Eqs. (30), (46), and (66).

Much simpler forms than for η^+ are obtained for the material functions $\Psi_1^+ = (\sigma_{xx} - \sigma_{yy})/\xi_0^2$ and $\Psi_2^- = -(\sigma_{yy} - \sigma_{zz})/\xi_0^2$. Both quantities do not depend on the shear rate to the order considered. The former shows a universal temporal behavior in units of its stationary value $\Psi_1 = K_1\tau^2$

$$\Psi_1^+(d)/K_1\tau^2 = \left[1 - (1+d)\,e^{-d}\right] + \mathcal{O}\left(\xi_0^2\right). \qquad (67)$$

As one can seen clearly in Fig. 10. there is in the present approximation no overshoot and Ψ_1^+ converges monotonically towards the stationary value Ψ_1.

The second material function depends on $K' \equiv K_2/K_1$

$$\begin{aligned}-4\Psi_2^+(d)/K_1\tau^2 &= 5 - K' - 2(4 + d - K')e^{-d} \\ &+ (3 - K')e^{-2d} + \mathcal{O}\left(\xi_0^2\right). \qquad (68)\end{aligned}$$

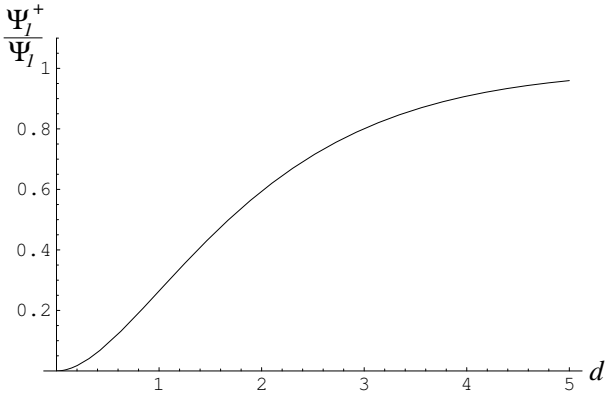

FIG. 10: *The material function Ψ_1^+ in units of Ψ_1 as a function of dimensionless time d.*

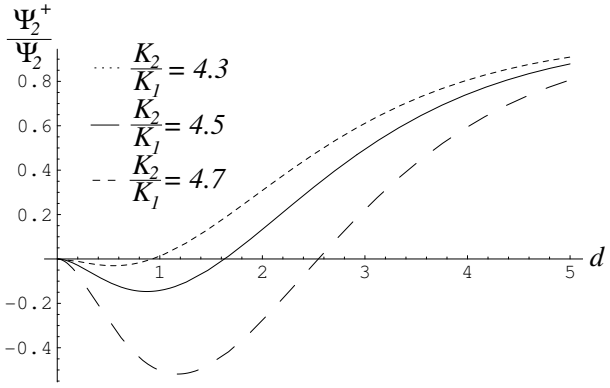

FIG. 11: *The material function Ψ_2^+ in units of Ψ_2 as a function of dimensionless time d for various values of K_2/K_1.*

Fig.11 reveals a negative dip of Ψ_2^+/Ψ_2 meaning that Ψ_2^+ becomes positive first, goes through a maximum and converges monotonically to the always negative stationary value Ψ_2 form Eq. (33). This is at least the case for values of K' within our limits $4 < K' < 5$. In addition, the time interval for which Ψ_2^+ is positive, becomes larger the larger K'. This property naturally influences also the ratio of Ψ_1^+ and Ψ_2^+ (Fig. 12), that becomes negative in the same time interval, where Ψ_2^+ is positive. Note, the limiting value for $d \to 0$ is physically irrelevant here. Our results show that the assumption [35], $\Psi_2^+/\Psi_1^+ = \Psi_2/\Psi_1$, is reasonable only for sufficiently large times.

E. Oscillatory shear flow

As a third example of a time-dependent shear flow with the geometry of Fig. 1 we discuss the case that the upper plate is oscillating with a frequency ω. The shear rate then takes the form

$$\dot\gamma(t) = \dot\gamma_0 \cos(\omega t)\ . \qquad (69)$$

$\dot\gamma_0$ is the amplitude of the oscillation, the frequency ω is chosen positive without loss of generality. The frequency

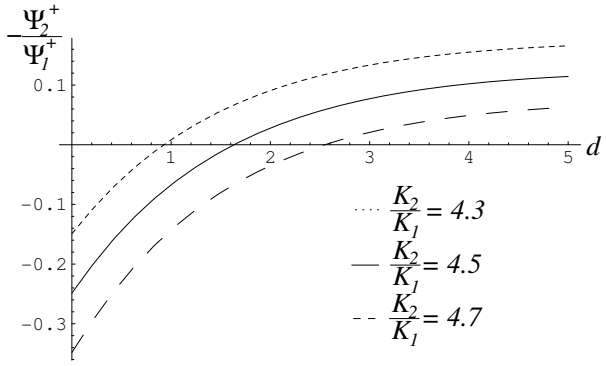

FIG. 12: *The ratio $-\Psi_2^+/\Psi_1^+$ as a function of dimensionless time d for different values of K_2/K_1.*

must satisfy the restriction

$$\omega \ll \frac{\eta_0}{\rho L^2} \tag{70}$$

so that the velocity profile can be considered to be linear [5]. To get a feeling for the order of magnitude, we estimate some typical numbers. With the smallest value of the viscosity coefficient from table I, $\eta_0 = 3 \cdot 10^2 \mathrm{Pa\,s}$, an estimated density of $\rho \approx 10^3 \mathrm{kg/m^3}$ and a distance between plates of 2 mm we find the restriction $\omega \ll 10^5 \mathrm{s}^{-1}$. In this connection we must keep in mind that the viscosity is in general a function of the shear rate; with the use of η_0 we assume automatically that we consider only small shear rates meaning also small amplitudes $\dot{\gamma}_0$. Our main interest in this section will be the discussion of linear viscoelasticity; in addition we want to see what our model predicts for the behavior of the normal stress differences.

The Eqs. (17)-(19) for the strain tensor U_{ij} read for the present case

$$\dot{U}_{xx} - \dot{U}_{yy} + U_{xx} - U_{yy} = 2\,\xi_0 \cos(\tilde{\omega} d)\, U_{xy} \tag{71}$$

$$\dot{U}_{xy} + U_{xy} = \xi_0 \cos(\tilde{\omega} d) \left(\frac{1}{2} - U_{xx} \right) \tag{72}$$

$$U_{xx} + U_{yy} = 2\,U_{xx} U_{yy} - 2\,U_{xy}^2. \tag{73}$$

Here we have introduced the dimensionless frequency $\tilde{\omega} = \omega\tau$, and the dimensionless amplitude of the shear rate, $\xi_0 = \dot{\gamma}_0 \tau$. The initial conditions do not need to be specified, since we are not interested in the onset behavior, but rather in the asymptotic state.

Again, it is nontrivial to solve these dynamic equations. But since the amplitude ξ_0 is a small quantity, we will use the following expansion

$$U_{xy}(\xi_0, d, \tilde{\omega}) = B_{xy}(\tilde{\omega}, d)\,\xi_0 + \mathcal{O}\left(\xi_0^3\right) \tag{74}$$

$$U_{xx}(\xi_0, d, \tilde{\omega}) = B_{xx}(\tilde{\omega}, d)\,\xi_0^2 + \mathcal{O}\left(\xi_0^4\right) \tag{75}$$

$$U_{yy}(\xi_0, d, \tilde{\omega}) = B_{yy}(\tilde{\omega}, d)\,\xi_0^2 + \mathcal{O}\left(\xi_0^4\right), \tag{76}$$

where the shear component is linear and the diagonal components are quadratic in ξ_0. In leading orders, we find the following solutions

$$B_{xy}(\tilde{\omega}, d) = \mathcal{A}_{xy}(\tilde{\omega}) \cos(\tilde{\omega} d + \varphi_{xy}(\tilde{\omega})) \tag{77}$$

$$B_{ii}(\tilde{\omega}, d) = \mathcal{V}_{ii}(\tilde{\omega}) + \mathcal{A}_{ii}(\tilde{\omega}) \cos(2\tilde{\omega} d + \varphi_{ii}(\tilde{\omega})), \tag{78}$$

with $i = x, y$. The amplitudes are

$$\mathcal{A}_{xy}(\tilde{\omega}) = \frac{1}{2\sqrt{1+\tilde{\omega}^2}} \tag{79}$$

$$\mathcal{A}_{xx}(\tilde{\omega}) = \frac{1}{8\,(1+\tilde{\omega}^2)} \frac{1}{\sqrt{1+4\tilde{\omega}^2}} \tag{80}$$

$$-\mathcal{A}_{yy}(\tilde{\omega}) = \frac{1}{8\,(1+\tilde{\omega}^2)} \sqrt{\frac{9+16\tilde{\omega}^2}{1+4\tilde{\omega}^2}} \tag{81}$$

$$\mathcal{V}_{xx}(\tilde{\omega}) = -\frac{1}{3}\mathcal{V}_{yy}(\tilde{\omega}) = \frac{1}{8\,(1+\tilde{\omega}^2)}, \tag{82}$$

and for the phase angles we get

$$\tan\varphi_{xy}(\tilde{\omega}) = -\tilde{\omega} \tag{83}$$

$$\tan\varphi_{xx}(\tilde{\omega}) = -\frac{2\tilde{\omega}\left(2-\tilde{\omega}^2\right)}{1-5\tilde{\omega}^2} \tag{84}$$

$$\tan\varphi_{yy}(\tilde{\omega}) = -\frac{2\tilde{\omega}\left(4+7\tilde{\omega}^2\right)}{3+\tilde{\omega}^2-8\tilde{\omega}^4}. \tag{85}$$

Thus, U_{xy} oscillates around the undeformed state $U_{xy} = 0$ with the same frequency as the upper plate, but with a phase shift φ_{xy}. The amplitude and the phase angle depend on $\tilde{\omega}$ and therefore on the frequency and the relaxation time. In contrast, the diagonal elements U_{xx} and U_{yy} show a completely different behavior. Both components oscillate with twice the frequency around a value different from zero $\mathcal{V}_{ii}$, which is a function of $\tilde{\omega}$ and which is different for U_{xx} and U_{yy}. The amplitudes $\mathcal{A}_{xx}$ and $\mathcal{A}_{yy}$ as well as the phase angles φ_{xx} and φ_{yy} are also different from each other.

Fig. 13 shows the behavior of the oscillation amplitudes $\mathcal{A}_{xy}$, $\mathcal{A}_{xx}$ and $\mathcal{A}_{yy}$. They are all monotonically decreasing functions of the frequency ω and of the relaxation time τ. We notice that $\mathcal{A}_{xy}$ has the highest amplitude. Since in addition the diagonal components of the strain tensor are by a factor ξ_0 smaller than the shear component, this means that the oscillation of the latter is, as a rule, at least one order of magnitude larger than that of the diagonal components.

In addition we note that $\mathcal{V}_{xx} > \mathcal{A}_{xx}$ as well as $|\mathcal{V}_{yy}| > |\mathcal{A}_{yy}|$. Therefore, the diagonal components do not change sign during the oscillations and we always have $U_{xx} > 0$ and $U_{yy} < 0$. The frequency dependence of the various phase angles becomes clear from Fig. 14. The phase shift is in general the larger, the higher the frequency or the longer the relaxation time.

For the shear stress σ_{xy} we find in linear order in ξ_0 the well-known linear viscoelastic form [5, 6]

$$\sigma_{xy} = -\left(\eta' \cos(\tilde{\omega} d) + \eta'' \sin(\tilde{\omega} d)\right) \frac{\xi_0}{\tau}, \tag{86}$$

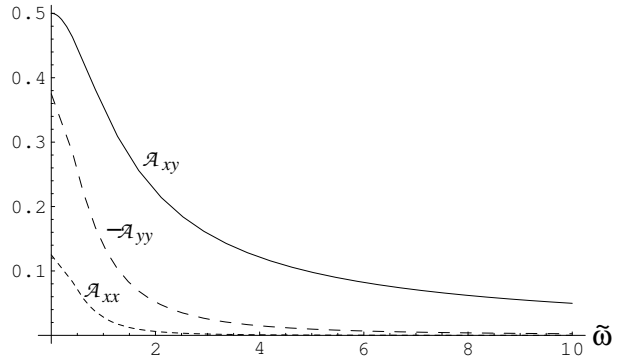

FIG. 13: *The amplitudes $\mathcal{A}_{xy}$, $\mathcal{A}_{xx}$ and $\mathcal{A}_{yy}$ are plotted ass functions of the dimensionless frequency $\tilde{\omega} = \omega\tau$.*

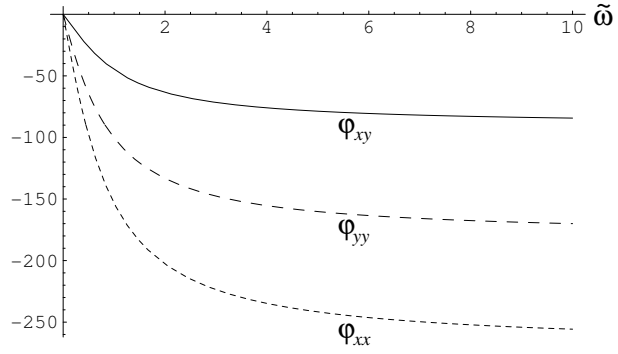

FIG. 14: *The phase angles φ_{xy}, φ_{xx} and φ_{yy} as a function of the dimensionless frequency $\tilde{\omega} = \omega\tau$.*

with

$$\eta' = \eta_\infty + \frac{K_1\tau}{2\left(1+\tilde{\omega}^2\right)} \tag{87}$$

$$\eta'' = \frac{K_1\tau\tilde{\omega}}{2\left(1+\tilde{\omega}^2\right)}. \tag{88}$$

Both quantities are independent of the oscillation amplitude and functions of the dimensionless frequency. The viscous part, η', is constant for vanishing frequency and monotonically drops to zero for very high frequency. The elastic contribution, η'', vanishes for both these limits and has a maximum in between at $\tilde{\omega} = 1$, allowing for an evaluation of the relaxation time τ. Often, the two functions are combined to a complex material function $\eta^* = \eta' - i\eta''$.

Written in the form of the strain components, $\sigma_{xy} = \mathcal{A}_{12}(\tilde{\omega})\xi_0\cos(\tilde{\omega}d + \varphi_{12}(\tilde{\omega}))$ we note that the phase angle here, φ_{12}, is different from the phase of the shear strain, φ_{xy}. However, $\tan\varphi_{xy} = \tan\varphi_{12}(1+\alpha[1+\tilde{\omega}^2])$, and the difference is negligibly small, since $\alpha \equiv 2\eta_\infty/\tau K_1 \ll 1$.

Qualitatively the behavior of η' as a function of frequency is reminiscent of the shear thinning of the stationary material function η as a function of shear rate. Indeed, W.P. Cox and E.H. Merz have found in 1958 from measured data the empirical relation [36]

$$\eta\left(\xi\right) = \left|\eta^\star\left(\tilde{\omega} = \xi\right)\right| \ , \tag{89}$$

which is known as Cox-Merz rule [5]. If one replaces the frequency in $|\eta^\star|$ by the shear rate, one obtains the viscosity of stationary shear flow, η as a function of shear rate. This relation is valid for a number of materials within the error bar of the measurements, for others this rule is a good approximation mainly for small shear rates [5]. This relation is rather remarkable, since $|\eta^\star|$ follows from a linear analysis, while shear thinning is an intrinsically nonlinear effect.

To investigate how well our model satisfies the Cox-Merz rule, we confine ourselves in the present paper to the case of small $\tilde{\omega}$. We therefore expand $|\eta^\star|$, the magnitude of the complex viscosity $\eta^\star$ up to second order in $\tilde{\omega}$, neglect the influence of η_∞ and obtain

$$|\eta^\star| = \frac{1}{2}K_1\tau - \frac{1}{4}K_1\tau\tilde{\omega}^2 + \mathcal{O}\left(\tilde{\omega}^4\right) \ . \tag{90}$$

The material function $\eta(\xi)$ of a stationary shear flow is given by Eq. (30). Neglecting also the constant η_∞ and making the replacement $\xi = \tilde{\omega}$, both functions are identical, provided the elastic constants satisfy

$$K_3 = 4K_2 - 4K_1. \tag{91}$$

In Sec. III C we have seen that the function η^- only relaxes faster with growing ξ_0, when the condition $K_3 > 4K_2 - 4K_1$ is satisfied. Eq. (91) means that the relaxation of η^- does not depend on ξ_0, at least up to order ξ_0^3. Thus, the Cox-Merz rule is marginally compatible with our admissible range for K_3, meaning it is only a good approximation within the framework of our model.

A similar relation as for $|\eta^\star|$ can also be formulated for η' [36]. Here one connects η' with the derivative of the shear stress for stationary shear with respect to the shear rate

$$\eta'\left(\tilde{\omega} = \xi\right) = -\frac{\partial\sigma_{xy}}{\partial\xi}\left(\xi\right). \tag{92}$$

From Eq. (26) we find in order ξ_0^2

$$-\frac{\partial\sigma_{xy}}{\partial\dot{\gamma}} = \left(\eta_\infty + \frac{1}{2}K_1\tau\right) + \frac{3}{8}\left(2K_1 - 4K_2 + K_3\right)\tau\xi^2, \tag{93}$$

while in order $\tilde{\omega}^2$ Eq. (87) gives

$$\eta' = \left(\eta_\infty + \frac{1}{2}K_1\tau\right) - \frac{1}{2}K_1\tau\tilde{\omega}^2. \tag{94}$$

Both expressions coincide for small $\xi = \tilde{\omega}$, if

$$K_3 = 4K_2 - \frac{10}{3}K_1. \tag{95}$$

This relation is fully compatible with the admissible range for K_3 and therefore, the empirical rule (92) is well satisfied.

The normal stress differences $N_1 = \sigma_{xx} - \sigma_{yy}$ and $N_2 = \sigma_{yy} - \sigma_{zz}$ in oscillatory shear reflect the behavior of the diagonal components of the strain tensor. They oscillate with twice the applied frequency around finite values, which are larger than the amplitudes of the oscillations, so that N_1 and N_2 do not change sign as a function of time and are always negative and positive, respectively. All amplitude decrease monotonically with increasing frequency.

Defining material functions by

$$N_1 = -\Psi_1^{\mathrm{V}}\xi_0^2 - \Psi_1'\xi_0^2\cos(\tilde{\omega}d) - \Psi_1''\xi_0^2\sin(\tilde{\omega}d)\,, \quad (96)$$

we find

$$\Psi_1^{\mathrm{V}} = \frac{K_1}{2(1+\tilde{\omega}^2)} \quad (97)$$

$$\Psi_1' = \frac{K_1(1-2\tilde{\omega}^2)}{2(1+\tilde{\omega}^2)(1+4\tilde{\omega}^2)} \quad (98)$$

$$\Psi_1'' = \frac{3K_1\tilde{\omega}}{2(1+\tilde{\omega}^2)(1+4\tilde{\omega}^2)}. \quad (99)$$

These material functions have been discussed already in the framework of various constitutive models [37]. With these models relationships between the three functions given above and the quantities η' and η'' have been found [37]

$$\tilde{\omega}\Psi_1^{\mathrm{V}}(\tilde{\omega}) = \eta''(\tilde{\omega}) \quad (100)$$

$$\tilde{\omega}\Psi_1'(\tilde{\omega}) = \eta''(2\tilde{\omega}) - \eta''(\tilde{\omega}) \quad (101)$$

$$\tilde{\omega}\Psi_1''(\tilde{\omega}) = \eta'(\tilde{\omega}) - \eta'(2\tilde{\omega})\,. \quad (102)$$

By inserting and checking one can easily show that the results of our calculations satisfy these relations exactly. Our model is therefore also in the present case in agreement with experimental results and other theories.

F. The Weissenberg effect

In the last two sections of this chapter we will deal with effects which appear in sheared fluids with a free surface. The best known example is the Weissenberg or rod-climbing effect [5, 38] (Fig. 15).

When a rod is inserted into a Newtonian fluid parallel to gravity and rotated, the free surface is curved downward near the rod. If the experiment is repeated with a polymeric liquid, one finds as a rule the opposite behavior: the fluid is climbing up the rod. The magnitude of this surface deformation is typically also much more pronounced than for Newtonian fluids.

To discuss this effect we consider the system depicted in Fig. 15: a cylindrical rod with radius R rotates with constant angular velocity Ω in a polymeric fluid, whose free surface extends to infinity and which is parallel to the $x-y$ plane at $\Omega = 0$. The fluid layer is assumed to be sufficiently deep so that the bottom has no influence on the surface. The rotation axis is taken to be the

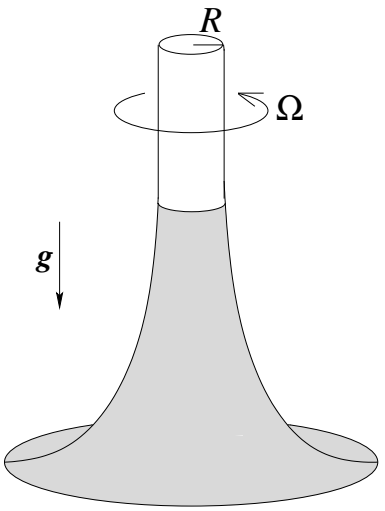

FIG. 15: *The principle of the Weissenberg effect: a polymeric fluid climbs up a rotating rod.*

z-axis, the direction of gravity is taken to be $-\hat{\mathbf{z}}$. In addition the rod is assumed to be so long that there are no boundary effects from the ends of the rod near the surface of the liquid. Since the system is rotationally symmetric around the z-axis, the use of cylindrical coordinates (r, φ, z) seems natural, in addition, we assume that the variables do not depend on φ. Furthermore we neglect a possible z-dependence. For the chosen system this implies that all frequency-dependent quantities can be expanded into powers of Ω and can be considered up to second order, since the z-dependence turns out to be a third order effect [39]. While the geometry does depend on z, this dependence can be expanded as a function of r and leads to a higher order effect [39]. The characteristic time scale which is given by the geometry of the system is

$$\tau_W = \sqrt{R/g}\,, \quad (103)$$

where g is the acceleration due to gravity. In a Newtonian fluid this is the only time scale; when we talk about small values of Ω, we mean that $\Omega\tau_{\mathrm{W}}$ is a small quantity. This means, for example, that for a rod with radius 1 cm we have $\tau_W = 3\cdot 10^{-2}$s and therefore we can consider in the expansion only angular velocities that are considerably smaller than $30\,\mathrm{s}^{-1}$. The thinner the rod, the larger the values for the angular velocities we can take care of. In a polymeric fluid we have the additional time scale τ, so that we have to discuss in detail later what we mean by small values of Ω.

To describe the deformation of the fluid surface one has to determine the surface profile $h(r)$, that is the height of the surface as a function of the distance from the central axis of the rod (cf. Fig. 16). The function $h(r)$ is determined up to an additive constant, since the depth of the fluid is unknown. Cylindrical coordinates are used.

A general, model-independent equation to determine

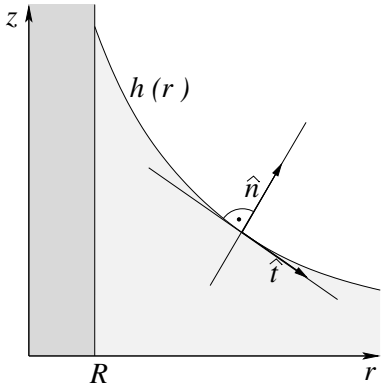

FIG. 16: *Cross section through the deformed surface for the Weissenberg- effect.* $h(r)$ *denotes the surface profile,* $\hat{\mathbf{t}}$ *is the tangential vector of the surface in the* r*-*z*-plane and* $\hat{\mathbf{n}}$ *is the normal vector.*

$h(r)$ has been derived in Refs. [5, 7] and reads

$$\rho g h(r) = \mathcal{C} + \rho \int_R^r \frac{v_\varphi^2}{r'}\,\mathrm{d}r' + \int_R^r \frac{N_1}{r'}\,\mathrm{d}r' - N_2, \qquad (104)$$

where $\mathcal{C}$ is a constant, v_φ is the azimuthal velocity component and N_1 and N_2 are the normal stress differences, which read for this geometry

$$N_1 = \sigma_{\varphi\varphi} - \sigma_{rr} \quad \text{and} \quad N_2 = \sigma_{rr} - \sigma_{zz}. \qquad (105)$$

We see that the surface profile has three contributions, namely a velocity dependent contribution, which also exists for Newtonian fluids, as well as one contribution each from N_1 and N_2.

Before we deal with polymeric fluids, we discuss first the behavior of a Newtonian fluid. In this case $\sigma_{ij}^{\mathrm{ela}} = 0$ and only the first integral in Eq. (104) contributes. The velocity profile follows from the Laplace equation with suitable boundary conditions in cylindrical geometry and reads

$$v_\varphi(r) = \frac{\Omega R^2}{r}. \qquad (106)$$

The magnitude of the velocity decreases radially with $1/r$. The surface profile, Eq. (104), reads in dimensionless form

$$\tilde{h}(r) = \tilde{h}_0 - \frac{(\Omega\,\tau_W)^2}{2\,\tilde{r}^2}, \qquad (107)$$

where all lengths with a tilde are scaled by R, e.g. $\tilde{r} = r/R$. We thus obtain the effect already described, namely that for a Newtonian fluid the surface at the rod curves downward with r^{-2}. As already mentioned this profile is only valid when the surface tension is neglected and under the condition that $\Omega\tau_W \ll 1$.

With our model we have the possibility to calculate the normal stress differences and therefore the surface profile of a polymeric fluid explicitly. To do this we will assume, as we have done before for all shear flow problems, that the velocity profile in a polymeric fluid coincides with the profile of a Newtonian fluid. Then we use Eqs. (2) and (1) to evaluate the strain field. Finally we have to examine the result obtained for consistency.

As before, we assume that the fluid is not stretched along its neutral direction, meaning that $U_{zz} = U_{zz}^0 = 0$. Then the determination of U_{ij} is reduced to a two-dimensional problem, this time in the r-φ-plane. In polar coordinates (r, φ) the dynamic Eqs. (2) and (1) for U_{ij} take the form

$$2\left(\nabla_r v_\varphi - \frac{v_\varphi}{r}\right) U_{r\varphi} = -\frac{1}{\tau}\left(U_{rr} - U_{\varphi\varphi}\right) \qquad (108)$$

$$2\left(\nabla_r v_\varphi - \frac{v_\varphi}{r}\right) U_{\varphi\varphi} = -\frac{2}{\tau} U_{r\varphi} + \nabla_r v_\varphi - \frac{v_\varphi}{r} \qquad (109)$$

$$U_{rr} + U_{\varphi\varphi} = 2\left(U_{rr}U_{\varphi\varphi} - U_{r\varphi}^2\right). \qquad (110)$$

Since the z-dependence of v_φ becomes important in third order in Ω, we can only expand the solution for U_{ij} up to second order and obtain

$$U_{r\varphi} = -\frac{\Omega\tau}{\tilde{r}^2} \qquad (111)$$

$$U_{\varphi\varphi} = -\frac{1}{3}U_{rr} = \frac{(\Omega\tau)^2}{\tilde{r}^4}. \qquad (112)$$

The small expansion parameter is $\Omega\tau \ll 1$. Since τ is in general larger than τ_W, the validity of the expansion is more restricted for a polymeric fluid than for a Newtonian fluid. As usual the diagonal components are even and the shear components odd functions of the shear direction, in this case given by the sign of Ω.

The non-vanishing components of the stress tensor can be calculated as usual and lead to the normal stress differences (up to order Ω^2)

$$N_1 = -4K_1\frac{(\Omega\tau)^2}{\tilde{r}^4} \qquad (113)$$

$$N_2 = (5K_1 - K_2)\,\frac{(\Omega\tau)^2}{\tilde{r}^4}. \qquad (114)$$

A comparison with the normal stress differences, which we have obtained for a stationary planar shear flow reveals that the solutions are identical when the shear rate is $\dot{\gamma} = -2\Omega/\tilde{r}^2$ in accordance with $\dot{\gamma} = \nabla_r v_\varphi$. The shear rate is therefore depending on location and falls off radially as r^{-2}. There is $N_1 < 0$ and $N_2 > 0$ also in the present case.

At this point we can check whether it was justified to take for a polymeric fluid the same velocity profile as for a Newtonian fluid. In order $(\Omega\tau)^2$ there is $\sigma_{r\varphi}^{\mathrm{ela}} \sim U_{r\varphi} \sim 1/r^2$. Therefore, the elastic part of the conservation equation for the φ-component of the momentum, $\nabla_r\,\sigma_{r\varphi}^{\mathrm{ela}} + (2/r)\sigma_{r\varphi}^{\mathrm{ela}}$, is identically zero. This leaves for the determination of $v_\varphi(r)$ only the Newtonian part.

We are now able to evaluate the surface profile in the limit $\Omega\tau \ll 1$. Inserting N_1 (eq.(113)), N_2 (eq.(114)) and

v_φ (eq.(106)) into Eq. (104) we have

$$\tilde{h}(\tilde{r}) = \tilde{h}_0 - \frac{\Omega^2 \tau_W^2}{2\tilde{r}^2} + \frac{K_2 - 4K_1}{\rho g R} \frac{\Omega^2 \tau^2}{\tilde{r}^4}. \qquad (115)$$

This result coincides formally with the result of Ref. [40], which has been obtained for a different model. In comparison to the Newtonian case, Eq. (107), the additional term due to the normal stress differences allows a rise of the fluid at the rod. The necessary condition for that is a positive prefactor of the new term, which requires

$$K_2 > 4K_1. \qquad (116)$$

Together with Eq. (34) this leads to an interval of admissible values for K_2, $4K_1 < K_2 < 5K_1$, resembling the similar condition for K_3 derived above. Relation (116) is compatible with the typical order of magnitude $K_2 \approx 4.5K_1$, which we have derived in Sec. III B. Using Eq. (33), we can express this condition in terms of the stationary normal stress differences, Ψ_1 and Ψ_2, that can be observed in stationary shear experiments

$$-\frac{\Psi_2}{\Psi_1} < 0.25, \qquad (117)$$

which allows for a prediction, whether a fluid can show the Weissenberg effect or not. In [7] this condition is also discussed. A survey for the values of these ratios for several samples can be found, for example in [7] in Table 3.9.

Eq. (115) shows that two different effects compete for the deformation of the surface. On the one hand there is a Newtonian contribution, which lowers the surface at the rod proportionally to r^{-2}, on the other hand a polymeric contribution, which raises the surface with the stronger dependence r^{-4}. To realize a rise of the liquid surface at the rod in experiments, $h(R)$ must be larger than h_0. This is the case for $R < R_{\rm crit}$ with

$$R_{\rm crit}^2 = \frac{2\,(K_2 - 4K_1)\,\tau^2}{\rho}, \qquad (118)$$

with the change of the height at the rod given by

$$\Delta h = h(R) - h_0 = \frac{R_{\rm crit}^2 - R^2}{2g}\Omega^2\ . \qquad (119)$$

The condition $R < R_{\rm crit}$ relates material properties with experimental geometric conditions. It comes in addition to Eq. (116), which only involves material properties. Such a supplementary condition is also discussed in Refs. [40] and [41].

In a Newtonian fluid the strength of the deformation Eq. (107) scales with Ω^2 and R^2, i.e. it is stronger for thicker rods and for higher rotation rates. For a polymeric fluid the situation is somewhat different, cf. Eq. (115). The elastic part of the deformation also scales with Ω^2, but is independent of the rod radius. Both contributions scale with the square of the respective relaxation time, which for the Newtonian effect is the geometric relaxation τ_W^2, and τ^2 for the elastic part. The more slowly the polymer relaxes, the larger is the Weissenberg effect. These results are based on a power expansion that is valid for $\Omega\tau \ll 1$ (and $\Omega\tau_{\rm W} \ll 1$). Taking into account additional effects neglected here, like surface tension, and for frequencies outside the validity range of the expansion, the Weissenberg effect shows a much more complex behavior [40], in particular the change of the height at the rod grows slower than Ω^2. In the present treatment we have focused on the fundamental mechanisms based on the intrinsic elasticity and its relaxation.

G. Flow through an inclined channel

As already mentioned the second normal stress difference for a shear flow is in magnitude much smaller than the first normal stress difference and therefore much harder to measure. In this section we want to examine a surface effect, which is determined exclusively by N_2 and therefore allows to measure this quantity [42]. The experimental set-up is presented in Fig. 17.

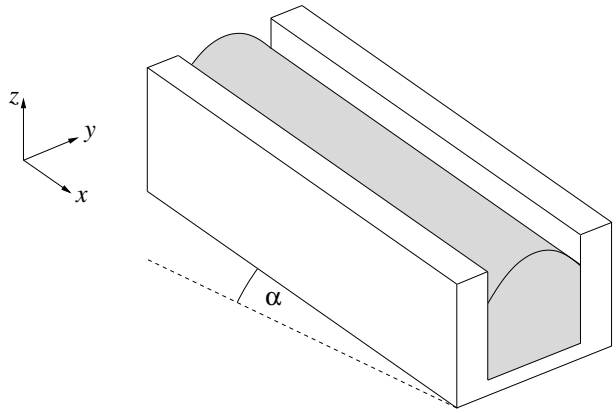

FIG. 17: *Flow of a polymeric fluid through a channel which is tilted by an angle α. The deformation of the surface is exaggerated for clarity.*

We consider a channel with a small inclination and parallel sidewalls in which the polymeric fluid flows. Experimentally it has been established [7], that the surface is curved weakly upwards, when the effect of surface tension is negligible. In contrast, for a Newtonian fluid a flat surface results. Fig. 18 shows the velocity profile.

We assume that the flow is laminar so that the velocity has only a x-component. In addition we consider a deep channel so that the flow velocity does not depend on the depth and is z independent. This assumption is justified by the fact that in the description of the experiments a deep channel is considered explicitly. In addition we consider a sufficiently long channel so that we can use translational symmetry along the x-axis. Therefore the velocity profile takes the form

$$\mathbf{v}\,(y) = v_x(y)\,\hat{\mathbf{x}}\ . \qquad (120)$$

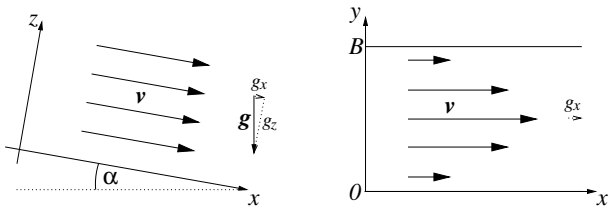

FIG. 18: *Structure of the flow profile in the x-z-plane (left) and in the x-y-plane (right).*

Thus, the present case also belongs to the class of stationary shear flows. The form of the y-dependence is sketched in the right plot of Fig. 18. Since the fluid is sticking at the channel walls, there are boundary conditions

$$v_x(0) = v_x(B) = 0 \; , \tag{121}$$

where B is the width of the channel. Since there is flow within the channel, the shear rate $\dot\gamma = \nabla_y v_x$ cannot be a constant, but is a function of y. Thus, we can take over all results from Sec. III B, where the space dependence of $\dot\gamma$ does not matter. This is the case for the derivation of the strain and stress tensor expressions.

The fluid is driven by gravity via $g_x = g \sin\alpha$ (left plot of Fig. 18), where generally α is small. The force balance for the x-direction therefore reads, cf. Eqs. (3) and (26)

$$\left[\eta_\infty + \frac{1}{2}K_1\tau + \frac{3}{8}\left(2K_1 - 4K_2 + K_3\right)\tau^3\dot\gamma^2\right]\nabla_y\dot\gamma = -\rho g \sin\alpha \; . \tag{122}$$

Since $\dot\gamma$ vanishes with α we will neglect the $\dot\gamma^2$ contributions and get, with the proper boundary conditions,

$$\dot\gamma(y) = \frac{\rho g\alpha}{2\eta_\infty + K_1\tau}\left(B - 2y\right) + \mathcal{O}\left(\alpha^3\right) \; . \tag{123}$$

The deformation of the surface is described by the profile $h(y)$, which arises by the intersection of the y-z-plane with the channel (Fig. 19). It is determined only up to

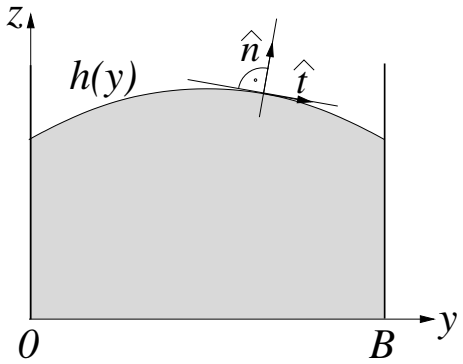

FIG. 19: *Profile $h(y)$ as well as normal- and tangential directions in the y-z-plane for a channel with width B.*

an additive constant, because of the unspecified depth. Similarly to the case of the Weissenberg-effect a model-independent equation for $h(y)$ can be derived [7]

$$\rho g h(y)\cos\alpha = \mathcal{C} - N_2, \tag{124}$$

where $N_2 = \sigma_{yy} - \sigma_{zz}$ is the second normal stress difference and $\mathcal{C}$ is the undetermined (irrelevant) constant. For a Newtonian fluid $N_2 = 0$ and h has to be constant, i.e. the surface is flat.

For the evaluation of N_2 we again can take over the solutions from Sec. III B

$$N_2 = \frac{1}{4}\left(5K_1 - K_2\right)\tau^2\dot\gamma^2 \; . \tag{125}$$

We now have all informations to calculate the surface profile

$$h(y) = h_0 + \frac{\rho g\alpha^2}{K_1}\left(5 - \frac{K_2}{K_1}\right)(B - y)y \; . \tag{126}$$

where h_0 is the undetermined constant and we have neglected η_∞ compared to $K_1\tau$. We thus find that the surface is curved upward parabolically and that the amplitude of the deformation grows quadratically in the tilt angle. The condition for giving the correct sign of the deformation, $K_2 < 5K_1$, is identical with the condition for $N_2 > 0$ used in Sec. III B. The deformation of the surface of shear flow in an inclined channel is qualitatively different from the deformation obtained for the Weissenberg-effect. In the present case the relaxation time τ has no influence on the deformation of the surface. In addition, a large K_1 and a small density reduce the deformation, while for the Weissenberg-effect the deformation grows with τ^2, is linear in the elastic constants and inversely proportional to ρ. Decisive for this qualitative difference is the structure of the velocity field. For the Weissenberg-effect it is completely determined by the geometry and contains only external parameters, namely the radius of the rod and its rotation frequency. Since for the channel the flow is driven by gravity, the velocity, Eq. (123), depends also on the material parameters.

IV. ELONGATIONAL FLOWS

Looking at various types of planar shear flows, we have noticed that in the limit of small deformations our model describes qualitatively very well the behavior of measurable quantities. To underline the importance of these results it is useful to investigate another type of flow, which has properties that are qualitatively different from those of shear flows. A natural candidate are three-dimensional elongational flows, which contain no shear component and show therefore a completely different behavior. We first present some general considerations and then address two specific experimental situations.

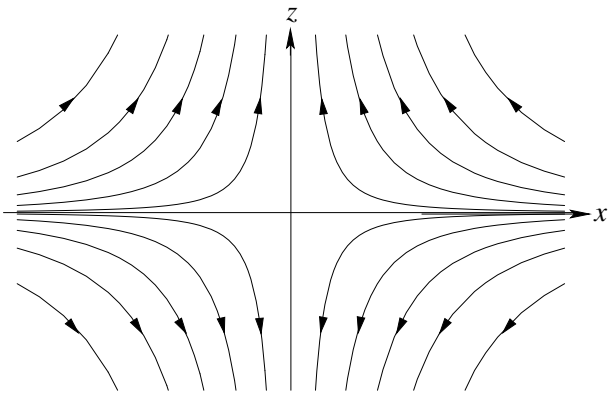

FIG. 20: *Three-dimensional elongational flow. The flow field is rotationally symmetric about the z−axis. The orientation of the stream lines is referring to* $\dot{\varepsilon} > 0$.

A. General considerations

Before we study concrete examples, we determine first the structure of the strain tensor and the dynamic equations for U_{ij}. As for the planar shear flow studied in III A we assume that the velocity profile is unchanged compared to that of a Newtonian fluid. The validity of this assumption is experimentally well confirmed [5]. The velocity profile of interest here takes the form

$$\mathbf{v}\left(\mathbf{r},t\right) = \begin{pmatrix} -(1/2)\dot{\varepsilon}\left(t\right)x \\ -(1/2)\dot{\varepsilon}\left(t\right)y \\ \dot{\varepsilon}\left(t\right)z \end{pmatrix}. \tag{127}$$

The flow is rotationally symmetric and incompressible. Its strength is determined by the elongation rate $\dot{\varepsilon}$, which is time-dependent, but spatially homogeneous.

Because of the symmetry of the flow, the laboratory system corresponds to the set of principal axes of A_{ij} as well as of U_{ij}. This is in contrast to the case of shear flow, where the set of principal axes of these two quantities was significantly different from the laboratory system as well as from each other. The strain tensor therefore takes the form

$$\mathbf{U} = \begin{pmatrix} U_{xx} & 0 & 0 \\ 0 & U_{yy} & 0 \\ 0 & 0 & U_{zz} \end{pmatrix}. \tag{128}$$

In addition, there is $U_{xx} = U_{yy}$, due to the rotational symmetry about the z-axis. Since we are already in the set of principal axes, we can give the stretch ratios directly

$$\lambda_1 = \frac{1}{\sqrt{1-2U_{xx}}} \quad \text{and} \quad \lambda_2 = \frac{1}{\sqrt{1-2U_{zz}}}. \tag{129}$$

When inserting the structure of U_{ij} into the equation of motion (2) we realize another difference to shear flow. While in III A the contribution $v_k \nabla_k U^0_{ij}$ is not allowed for symmetry reasons, it contributes in the present case. Therefore, the equations of motion represent a system of partial differential equations, which is nontrivial to solve. We circumvent this problem by assuming that the strain field is spatially homogeneous. This assumption is supported by the fact that the elongation rate is also spatially homogeneous. Every component of Eq. (2) yields the same equation

$$\left(\frac{1}{\tau} + \frac{\partial}{\partial t}\right)\left(U_{xx} - U_{zz}\right) + \frac{3}{2}\dot{\varepsilon} = U_{xx} + 2U_{zz}. \tag{130}$$

As before for shear flow, we will work here with dimensionless quantities and define

$$\zeta \equiv \dot{\varepsilon}\tau \quad \text{and} \quad d \equiv \frac{t}{\tau}, \tag{131}$$

where ζ is, in analogy to ξ, the dimensionless elongation rate, d, we know already from III A. Including the incompressibility condition, Eq. (1), the system of equations we will analyze in the following takes the form

$$\dot{U}_{xx} - \dot{U}_{zz} + (1-\zeta)\,U_{xx} - (1+2\zeta)\,U_{zz} = -\frac{3}{2}\zeta \tag{132}$$

$$\left(1-2U_{xx}\right)^2\left(1-2U_{zz}\right) = 1, \tag{133}$$

where from now on the dot refers to time derivatives with respect to d.

Starting from Eqs. (132) and (133) we will now discuss two scenarios, namely stationary elongational flow and the onset of elongational flow.

B. Stationary elongational flow

While there are three different measurable quantities in a shear flow, the situation in a rotationally symmetric elongational flow is simpler. Because of the high symmetry there is only one measurable quantity namely the normal stress difference $\sigma_{zz} - \sigma_{xx}$ [5]. In this section we want to study the behavior of this quantity in a stationary flow. The elongation rate is constant in this case,

$$\dot{\varepsilon} = \text{const.}\,, \tag{134}$$

and also the strain components are time-independent. Such a flow is experimentally difficult to realize (cf., e.g. Ref. [43]) and only for small elongation rates ($\dot{\varepsilon} < 1 - 10s^{-1}$); larger values can be investigated for the onset of elongational flow.

The stationary solution of Eqs. (132) and (133) is simple to determine and takes the form

$$2\mathbf{U} = \mathbf{I} - \begin{pmatrix} \left(\frac{1+2\zeta}{1-\zeta}\right)^{1/3} & 0 & 0 \\ 0 & \left(\frac{1+2\zeta}{1-\zeta}\right)^{1/3} & 0 \\ 0 & 0 & \left(\frac{1-\zeta}{1+2\zeta}\right)^{2/3} \end{pmatrix}, \tag{135}$$

with $\mathbf{I}$ the unit tensor. As for the strain tensor of a stationary shear flow, U_{ij} is universal, since there is only a dependence on ζ. We note that the strain has singularities for $\zeta_1 = -\frac{1}{2}$ and $\zeta_2 = 1$ and a stationary elongational flow is only possible for

$$-\frac{1}{2\tau} < \dot{\varepsilon} < \frac{1}{\tau}. \tag{136}$$

This provides a possible explanation for the experimental restriction to small elongation rates. Such a restriction is also found in various other approaches [7, 44]. This regime of existence becomes larger the faster the fluid relaxes.

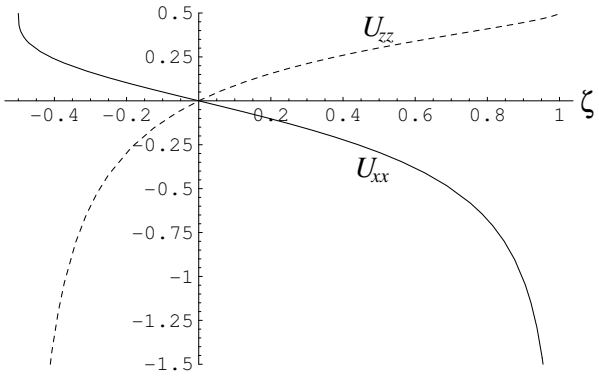

FIG. 21: *The strain components U_{xx} and U_{zz} of a stationary elongational flow are plotted as a function of the dimensionless elongation rate ζ.*

The other properties of the strain tensor can be seen in Fig. 21. There is no symmetry with respect to the sign of ζ. For a uniaxial extensional flow ($\dot{\varepsilon} > 0$) the system expands in z-direction ($U_{zz} > 0$) and it is compressed ($U_{xx} < 0$) in all perpendicular directions. The magnitude of the strain grows monotonically with ζ and reaches for $\zeta = 1$ the location where the strain diverges. For biaxial extensional flows ($\dot{\varepsilon} < 0$) the behavior is reverse. The fluid is strained in all directions perpendicular to the z-axis ($U_{xx} > 0$) and compressed in z-direction ($U_{zz} < 0$). The strain is growing monotonically with larger values of $|\zeta|$, but reaches already at $|\zeta| = 1/2$ the singularity of infinitely large strain.

The stretch coefficients λ_1 and λ_2 according to (129) assume the simple form

$$\lambda_1 = \left(\frac{1-\zeta}{1+2\zeta}\right)^{1/6} \quad \text{and} \quad \lambda_2 = \left(\frac{1+2\zeta}{1-\zeta}\right)^{1/3}. \tag{137}$$

It is worth to notice that the divergence at the boundary of the realizable regime shows a power law behavior: $\lambda_1 \sim (1+2\zeta)^{-1/6}$ near $\zeta = -\frac{1}{2}$ and $\lambda_2 \sim (1-\zeta)^{-1/3}$ near $\zeta = 1$.

To study the stresses appearing in an elongational flow we carry out an expansion in powers of ζ, since U_{xx} and U_{zz} are small quantities, when ζ is also small, cf. Fig. 21. Since ζ is within the rather narrow range between $-1/2$ and 1, such an expansion will be a good approximation except for the boundary regime where the information about the divergence is lost. The strain tensor takes then the form up to order ζ^3

$$\mathbf{U} = \begin{pmatrix} -\frac{1}{2}\zeta - \frac{1}{3}\zeta^3 & 0 & 0 \\ 0 & -\frac{1}{2}\zeta - \frac{1}{3}\zeta^3 & 0 \\ 0 & 0 & \zeta - \frac{3}{2}\zeta^2 + \frac{8}{3}\zeta^3 \end{pmatrix}. \tag{138}$$

In leading order the diagonal components are linear in ζ, in contrast to shear flow, where the diagonal components can only be functions of ξ^2.

For the evaluation of the stress tensor we make again use of Eqs. (5) and (9) and obtain up to third order in ζ:

$$\begin{aligned} \sigma_{xx} = \sigma_{yy} &= -\frac{\eta_\infty}{\tau}\zeta + \frac{1}{2}K_1\zeta + \frac{1}{4}(2K_1 - K_2)\zeta^2 \\ &\quad + \frac{1}{24}(8K_1 - 6K_2 + 3K_3)\zeta^3 \qquad (139) \\ \sigma_{zz} &= 2\frac{\eta_\infty}{\tau}\zeta - K_1\zeta + \frac{1}{2}(7K_1 - 2K_2)\zeta^2 \\ &\quad + \frac{1}{3}(-26K_1 + 15K_2 - 3K_3)\zeta^3. \qquad (140) \end{aligned}$$

The material function, which is connected with the normal stress difference $\sigma_{zz} - \sigma_{xx}$ in an elongational flow, is the Trouton- or elongational viscosity $\bar{\eta}$ [5]

$$\bar{\eta}(\dot{\varepsilon}) = -\frac{\sigma_{zz} - \sigma_{xx}}{\dot{\varepsilon}}. \tag{141}$$

While it is constant in a Newtonian fluid, it is a function of the elongation rate in a polymeric fluid. In our model we find

$$\begin{aligned} \bar{\eta} &= 3\left(\eta_\infty + \frac{1}{2}K_1\tau\right) + \frac{3}{4}(-4K_1 + K_2)\tau\zeta \\ &\quad + \frac{3}{8}(24K_1 - 14K_2 + 3K_3)\tau\zeta^2 + \mathcal{O}\left(\zeta^3\right). \qquad (142) \end{aligned}$$

As it is known [5, 45], for $\zeta \to 0$ the Trouton viscosity, $\bar{\eta}(\zeta \to 0) \equiv \bar{\eta}_0 = 3(\eta_\infty + 1/2K_1\tau)$, corresponds to three times the value of the shear viscosity for $\xi \to 0$. A comparison of (30) and (142) shows, that our model satisfies this property.

Since $K_2 > 4K_1$, Eq.(116), the linear part of $\bar{\eta}(\zeta)$ is positive. This means that for small $\zeta \ll 1$ the Trouton viscosity increases for a uniaxial elongational flow, and decreases with the magnitude of the elongation rate for biaxial elongation, which is in agreement with experiments [5, 46]. For larger magnitudes of ζ an increase of the viscosity is observed leading to a minimum [46]. In our expression this is taken care of by the quadratic term $\sim \zeta^2$. Indeed, it is positive, since

$$24K_1 - 14K_2 + 3K_3 > 2(6K_1 - K_2) > 0, \tag{143}$$

where we have made use of the inequalities $K_2 < 5K_1$, Eq .(34), and $K_3 > 4K_2 - 4K_1$, Eq. (50). Fig. 22 shows this behavior using our standard values for the elastic constants. Of course, the steep increase of the Trouton

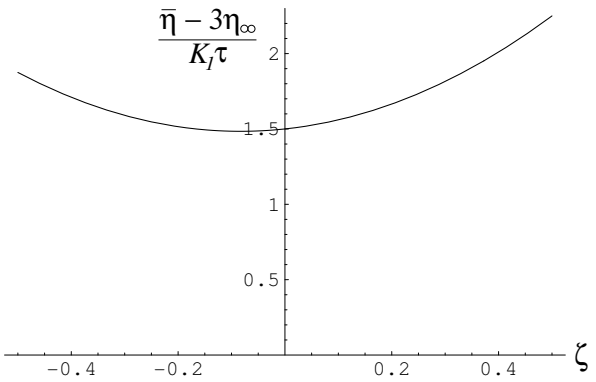

FIG. 22: *The Trouton viscosity $\bar{\eta}$ in units of $K_1\tau$ as a function of ζ for $K_2 = 4.5K_1$ and $K_3 = 15K_1$.*

viscosity observed near the singularities cannot be covered by this expansion approach and we have to refer to the companion paper (II) for further discussions.

The location of the minimum is given by

$$\zeta_{\min} = -\frac{-4K_1 + K_2}{24K_1 - 14K_2 + 3K_3}, \tag{144}$$

which gives $\zeta_{\min} = -0.083$ with the values used for Fig.22. Thus the minimum lies in a regime for which the approximation of small elongation rates is still valid.

C. The onset of elongational flow

As a last example we consider the onset behavior of an elongational flow. In this case the elongation rate takes the form

$$\dot{\varepsilon}(t) = \begin{cases} 0 & \text{for } t < 0 \\ \dot{\varepsilon}_0 & \text{for } t \geq 0 \end{cases}. \tag{145}$$

We proceed here in close analogy to the treatment of the onset of a shear flow. Especially interesting in this connection is the fact that one can choose elongation rates for which there is no stationary solution according to the last section. Since we consider first the limit of small elongation rates, we will discuss in this section only cases for which a stationary state exists. For the treatment of large elongation rates we refer to the companion paper (II).

To evaluate the strain tensor we must first solve the system of dynamic equations for U_{ij}, Eqs. (132) and (133), with ζ_0 replacing ζ, together with the initial conditions

$$U_{xx}(\zeta_0, d=0) = U_{zz}(\zeta_0, d=0) = 0, \tag{146}$$

where we have used the notation $\zeta_0 = \dot{\varepsilon}_0\tau$. Although this system of equations appears to be much simpler than that for the onset of shear flow, we have to use an expansion in powers of ζ. For the purposes of this section we need, however, this expansion only up to order ζ_0^3

$$U_{xx}(\zeta_0, d) = a_x(d)\,\zeta_0 + b_x(d)\,\zeta_0^2 + c_x(d)\,\zeta_0^3 \tag{147}$$
$$U_{zz}(\zeta_0, d) = a_z(d)\,\zeta_0 + b_z(d)\,\zeta_0^2 + c_z(d)\,\zeta_0^3. \tag{148}$$

Since there are no symmetries for the elongational flow with respect to the elongation rate, all orders contribute. Inserting this expansion into the system of equations and comparing coefficients, leads to six equations for the six time dependent expansion coefficients, which can be solved analytically. The expressions obtained are rather involved and will not be shown here.

From the calculated components of the strain tensor, we obtain using Eq. (129) the stretch ratios λ_1 and λ_2, again as an expansion in ζ_0 up to third order

$$\lambda_1(\zeta_0, d) = 1 + \frac{1}{2}\left(e^{-d} - 1\right)\zeta_0 + \Gamma_{12}\zeta_0^2 + \Gamma_{13}\zeta_0^3 \tag{149}$$
$$\lambda_2(\zeta_0, d) = 1 + \left(1 - e^{-d}\right)\zeta_0 + \Gamma_{22}\zeta_0^2 + \Gamma_{23}\zeta_0^3, \tag{150}$$

with the abbreviations

$$\begin{aligned}
\Gamma_{12} &= \frac{3}{8} - \frac{1}{4}(1+2d)\,e^{-d} - \frac{1}{8}\,e^{-2d} \\
\Gamma_{13} &= -\frac{31}{48} + \frac{1}{16}\left(-5 + 20d + 4d^2\right)e^{-d} \\
&\quad + \frac{1}{16}(17 + 4d)\,e^{-2d} - \frac{5}{48}e^{-3d} \\
\Gamma_{22} &= (-1+d)\,e^{-d} + e^{-2d} \\
\Gamma_{23} &= \frac{2}{3} + \frac{1}{2}\left(2 - 2d - d^2\right)e^{-d} \\
&\quad - (1+2d)\,e^{-2d} - \frac{2}{3}e^{-3d}.
\end{aligned}$$

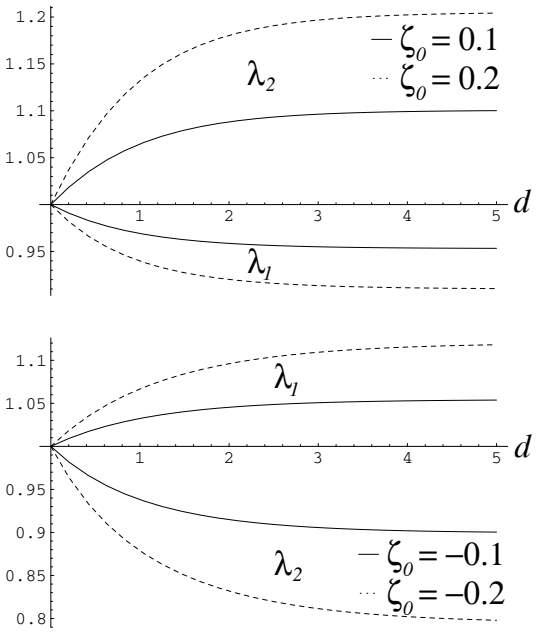

FIG. 23: *The stretch coefficients λ_1 and λ_2 as a function of dimensionless time d for uniaxial elongation flow (top) and biaxial elongation flow (bottom).*

λ_1 and λ_2 are plotted as a function of time for several values of ζ_0 in Fig. 23. For all values of the elongation rate shown both stretch ratios converge monotonically to their stationary value.

The material function $\bar{\eta}^+$ is defined as [5]

$$\bar{\eta}^+ (\dot{\varepsilon}_0, t) = -\frac{\sigma_{zz} - \sigma_{xx}}{\dot{\varepsilon}_0} \,, \tag{151}$$

where $t \geq 0$. Using the same approach as for the stretch coefficients we obtain

$$\bar{\eta}^+ = 3\eta_\infty + \frac{3}{2}\left(1 - e^{-d}\right) K_1\tau + \frac{3}{4}\Gamma_6\tau\zeta_0 + \frac{3}{8}\Gamma_7\tau\zeta_0^2, \tag{152}$$

with the abbreviations

$$\begin{aligned}
\Gamma_6 &= -4K_1 + K_2 + 2[(3+d)K_1 - K_2]e^{-d} \\
&\quad - (2K_1 - K_2)\, e^{-2d} \\
\\
\Gamma_7 &= 24K_1 - 14K_2 + 3K_3 - [\left(44 + 20d + 2d^2\right) K_1 \\
&\quad - (38 + 4d)\, K_2 + 9K_3]e^{-d} \\
&+ \left[(36 + 8d)\, K_1 - (34 + 4d)\, K_2 + 6K_3\right] e^{-2d} \\
&- \left(8K_1 - 10K_2 + 3K_3\right) e^{-3d}.
\end{aligned}$$

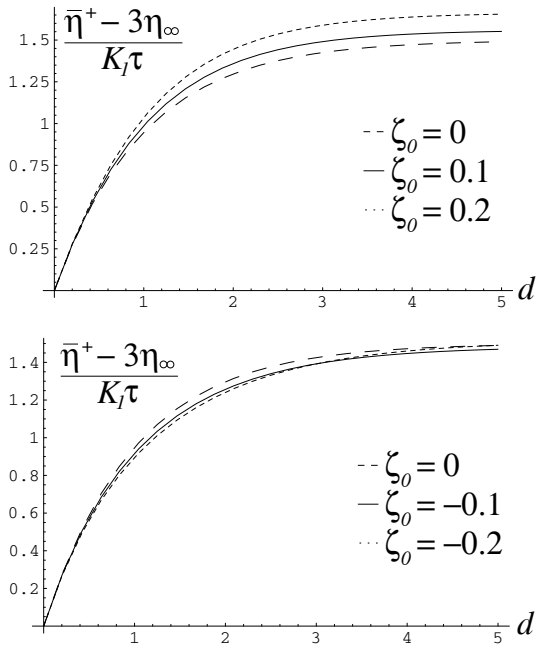

FIG. 24: *The Trouton viscosity $\bar{\eta}^+$ is plotted as a function of dimensionless time d for uniaxial elongation flow (top) and biaxial elongation flow (bottom). The limiting zero-elongation curve is shown in both parts to facilitate their comparison. We have used $K_2 = 4.5K_1$ and $K_3 = 15K_1$.*

The behavior of this function of time is plotted in Fig. 24, separately for uniaxial (top) and biaxial (bottom) elongation. For $d \to \infty$, the Trouton viscosity $\bar{\eta}^+$ approaches strictly monotonically its stationary value, $\bar{\eta}$, which is dependent on ζ (cf. Fig. 22). For the biaxial elongational flow the stationary Trouton viscosity has a minimum. In particular, $\bar{\eta}(\zeta = 0) > \bar{\eta}(\zeta = -0.1) < \bar{\eta}(\zeta = -0.2)$, which leads to an intersection of $\bar{\eta}^+(d)$ for $\zeta_0 = -0.1$ and $\zeta_0 = -0.2$ in the bottom of Fig. 24. This intersection is also found in experimental data [5].

The limiting zero-elongation curve $\bar{\eta}_0^+(d) \equiv \bar{\eta}^+(\zeta_0 = 0, d) = 3\eta_\infty + (3/2)(1 - e^{-d})K_1\tau$ is related to the limiting zero-shear curve for the onset of a shear flow, $\eta_0^+(d)$, Eq. (66). Both functions differ only by a factor of 3, a result that already follows from linearized elasticity theory [5]. Of course, this property is correctly derived also in our framework.

Acknowledgments: H.R.B. and H.P. acknowledge partial support of their work by the Deutsche Forschungsgemeinschaft through SPP 1681 'Feldgesteuerte Partikel-Matrix-Wechselwirkungen: Erzeugung, skalenübergreifende Modellierung und Anwendung magnetischer Hybridmaterialien'.

V. APPENDIX: DERIVATION OF THE POLYMERIC HYDRODYNAMICS

Starting from the equations as derived in Refs. [13, 15, 16], we shall simplify them to obtain those given in section II. The starting equations are rather general. They contain many aspects not of direct importance for the applications considered in this paper. In particular, we want to focus on the more essential features, especially the nonlinear influence of the strain tensor U_{ij}, while neglecting that of temperature and density gradients.

We use the Eulerian strain tensor, the variable part of the Cauchy strain [7], $C_{ij} = \delta_{ij} - 2U_{ij}$. In the absence of any deformation, U_{ij} is zero. The Gibbs-Duhem relation [4, 23–25], valid in local equilibrium, reads

$$\mathrm{d}\varepsilon = T\mathrm{d}s + \mu\mathrm{d}\rho + v_i\mathrm{d}g_i + \psi_{ij}\mathrm{d}U_{ij}, \tag{153}$$

where ψ_{ij} is the elastic stress to lowest order in U_{ij}, and $\psi_{ij} \equiv 0$ in equilibrium. All other quantities have the same meaning as for a simple fluid [1, 4].

The elastic strain tensor obeys [13, 16]

$$\dot{U}_{ij} + v_k\nabla_k U_{ij} - A_{ij} + U_{kj}\nabla_i v_k + U_{ik}\nabla_j v_k = X_{ij}^{\mathrm{D}}. \tag{154}$$

Note the relaxation term X_{ij}^{D} that is absent in an elastic system. This quasi-current X_{ij}^{D} vanishes in the high frequency (solid) limit and, at small frequencies (liquid limit), becomes so large that U_{ij} relaxes infinitely fast to zero and is no longer a variable.

A first simplification is incompressibility. The mass density ρ will be assumed to be constant from now on. Therefore mass conservation [1] is reduced to $\nabla_k v_k = A_{kk} = 0$. It is important to keep in mind that this assumption does *not* imply $U_{kk} = 0$. We note that the

strain tensor is solenoidal only at small strains. The conservation of momentum density then simplifies to

$$\rho\left(\dot{v}_i + v_k\nabla_k v_i\right) + \nabla_i P + \nabla_j \sigma_{ij} = 0, \tag{155}$$

where $P \equiv -\varepsilon^{\rm rf} + Ts + \mu\rho$ is the pressure and σ_{ij} is the elastic stress tensor of the system.

Another important simplification is the restriction to isothermal systems. Thus the temperature gradients throughout the fluid vanish and the temperature dependence of the material parameters is discarded. The entropy balance then takes the form

$$\dot{s} + v_k\nabla_k s = R/T\ , \tag{156}$$

and is no longer of interest in the following.

For the dissipative parts of the currents $\sigma_{ij}^{\rm D}$ and $X_{ij}^{\rm D}$ we have in the incompressible limit

$$\sigma_{ij}^{\rm D} = 2\eta_\infty A_{ij}^0 + 2\beta_1\psi_{ij}, \tag{157}$$

$$X_{ij}^{\rm D} = -2\alpha_1\psi_{ij}^0 - \alpha_2\psi_{kk}\delta_{ij} + 2\beta_1 A_{ij}^0, \tag{158}$$

where a superscript 0 denotes the traceless part of that quantity. The parameters $\alpha_{1,2}$ and η_∞ must all be positive. So far there is no experimental information about the magnitude of the cross-coupling parameter β_1. To keep the number of parameters as small as possible we will therefore take $\beta_1 = 0$ in the following. Should we find out that important effects cannot be described this way, we can still incorporate β_1 later.

Inserting the quasi-current $X_{ij}^{\rm D}$ into the dynamic equation for U_{ij}, Eq. (154), we realize that the resulting equation is difficult to solve: The elastic stress tensor ψ_{ij} is in general a nontrivial and as yet unspecified nonlinear function of U_{ij}, so is $\alpha_1(U_{ij})$. For simplicity we assume (1) $\psi_{ij}^0/|\psi_{ij}^0| = U_{ij}^0/|U_{ij}^0|$, or $\alpha_1(U_{ij})\psi_{ij}^0 = \alpha_1|\psi_{ij}^0|U_{ij}^0/|U_{ij}^0| = U_{ij}^0/\tau$, with (2) τ a constant. Hence, for the traceless part,

$$\dot{U}_{ij}^0 + v_k\nabla_k U_{ij}^0 - A_{ij}^0 + \left[U_{kj}\nabla_i v_k + U_{ik}\nabla_j v_k\right]^0 = -U_{ij}^0/\tau, \tag{159}$$

with τ accounting for the relaxation of shear deformations. By introducing the relaxation time τ we can quantify the viscoelastic behavior: if for an external perturbation the frequency ω obeys the inequality $\omega\tau \ll 1$, then the system behaves like a Newtonian fluid, while for $\omega\tau \gg 1$ it behaves like an elastic solid. Even for the second case, we have to make sure that the condition of validity for hydrodynamics $\omega\tau_{lg} \ll 1$ (with τ_{lg} the time scale to reach local equilibrium) is still satisfied. Since we want to have a consistent nonlinear elastic description in the solid limit, we will not make use of the condition, $U_{kk} = 0$. The general nonlinear incompressibility condition for U_{ij} requires the determinant of the Cauchy tensor C_{ij} to be unity [7]. In the system of principal axes of U_{ij} this relation can be written as

$$\left(1-2U_1\right)\left(1-2U_2\right)\left(1-2U_3\right) = 1, \tag{160}$$

where U_1, U_2 and U_3 are the eigenvalues of U_{ij}. Eq. (160) connects the six components of U_{ij}. It can be cast into the form $U_{kk} = f(U_{ij}^0)$, where f is, in general, a rather complicated function that vanishes, if linearized in U_{ij}^0, and if $U_{ij}^0 \to 0$. Here we present the explicit result for two dimensions, since for the examples considered in the bulk part of the paper either a two-dimensional description is used (shear flow, Weissenberg effect, flow through an inclined channel) or U_{ij} is diagonal in three dimensions (elongational flow) from the beginning. For the two-dimensional case we find

$$U_{kk} = 1 - \left[1 + 4U_{xy}^2 + 4(U_{xx}^0)^2\right]^{1/2} \tag{161}$$

We assume that this condition holds on the relevant time scale τ for the U_{ij}^0 dynamics. Therefore, $X_{ij}^{\rm D}$ is of the general form

$$X_{ij}^{\rm D} = -\frac{1}{\tau}U_{ij}^0 - \frac{1}{\hat{\tau}}\left(U_{kk} - f\left(U_{ij}^0\right)\right)\delta_{ij}, \tag{162}$$

with the volume relaxation time $\hat{\tau} = 1/\left(3\alpha_2 k_2\right)$ much shorter than τ; k_2 is the linear bulk elastic modulus. This representation does not contradict the equilibrium condition $\psi_{ij} = 0$, i.e. $U_{ij} = 0$. Within the approximation $\tau \gg \hat{\tau}$, the strain tensor U_{ij} is described by Eqs. (159) and (160).

Finally we must come back to the problem of calculating ψ_{ij}. For the contribution to $X_{ij}^{\rm D}$ we have linearized this quantity, but as already mentioned the nonlinearities of the elasticity are decisive for polymeric behavior. Since we cannot calculate the stress tensor σ_{ij} without specification of ψ_{ij}, we have to make a concrete assumption about the form of the elastic free energy. A rather natural approach is to expand the elastic contribution of the energy density into powers of U_{ij} and then to calculate ψ_{ij} from this expansion. This step naturally reduces the validity of the model for cases in which U_{ij} is a small quantity. With the possibility of a generalization to large deformations we will deal in the companion paper (II).

To construct an expansion of ε, we start with Eq. (153) and go to the rest system with the transformation $\varepsilon^{\rm rf} = \varepsilon - 1/2\rho v_i^2$. This energy density depends only on ρ, s and U_{ij} and will now be expanded into powers of U_{ij}. Since the elastic energy is independent of rotations of the coordinate system, only the three invariants of U_{ij} contribute. We can therefore expand $\varepsilon^{\rm rf}$ into the three eigenvalues U_1, U_2 and U_3, but prefer here the trace of U_{ij}, $\mathrm{Tr}\left(\mathbf{U}\right) \equiv U_{kk}$, as well as the traces of the squares of the second and third powers of U_{ij}, $\mathrm{Tr}\left(\mathbf{U}^2\right) \equiv U_{kl}U_{kl}$ and $\mathrm{Tr}\left(\mathbf{U}^3\right) \equiv U_{kl}U_{lm}U_{mk}$. It will become clear later in this paper that it is sensible to expand up to fourth order in U_{ij}

$$\varepsilon^{\rm rf}\left(s,\rho,U_{ij}\right) = \bar{\varepsilon}\left(s,\rho\right) + K_1\mathrm{Tr}\left(\mathbf{U}^2\right)/2 + K_2\mathrm{Tr}\left(\mathbf{U}^3\right)/3 + K_3\mathrm{Tr}\left(\mathbf{U}^4\right)/4. \tag{163}$$

Since U_{kk} is zero in linear order, it has to be at least of $O(2)$. Therefore, there is only one term in quadratic and

cubic order, each. The two possible fourth order terms, $\mathrm{Tr}\left(\mathbf{U}^4\right)$ and $\left(\mathrm{Tr}\left(\mathbf{U}^2\right)\right)^2$ give rise to only one additional coefficient, since $2\mathrm{Tr}(\mathbf{U}^4) = (\mathrm{Tr}(\mathbf{U}^2))^2$ [27]. As a result, there are only three elastic parameters K_1, K_2 and K_3. In principle, they can be functions of s and ρ, which plays, however, no role for our considerations. The linear elasticity constants used before can be represented by $k_1 = K_1$ and $k_2 = 1/3K_1$. To guarantee that the energy is minimum in the undeformed state, K_1 must be positive. ψ_{ij} can now be calculated up to third order

$$\psi_{ij} = K_1 U_{ij} + K_2 U_{ik}U_{kj} + K_3 U_{ik}U_{kl}U_{lj}. \qquad (164)$$

The elastic stress tensor is generally given as [17]

$$\sigma_{ij}^{\mathrm{ela}} = -\psi_{ij} + \psi_{ki}U_{jk} + \psi_{kj}U_{ik}. \qquad (165)$$

This expression is completely fixed by the dynamic strain equation, because of the zero entropy condition. Only in linear approximation does $\sigma_{ij}^{\mathrm{ela}} = -\psi_{ij}$ hold. With the result for ψ_{ij} we get

$$\begin{aligned}\sigma_{ij}^{\mathrm{ela}} = \quad & -K_1 U_{ij} + (2K_1 - K_2)\, U_{ik}U_{kj} \\ & + (2K_2 - K_3)\, U_{ik}U_{kl}U_{lj}. \end{aligned} \qquad (166)$$

We have now achieved a simplification of the hydrodynamic model for polymeric fluids, which is amenable to an analytic or almost analytic description of elementary types of flows. The important equations are the dynamic equations for U_{ij}, Eq. (159) (with the incompressibility (160)), as well as the conservation of momentum density (155) and the contributions to the stress tensor $\sigma_{ij} = \sigma_{ij}^{\mathrm{ela}} + \sigma_{ij}^{\mathrm{D}}$, Eqs. (166) and (157) (with $\beta_1 = 0$).

The simplified model has a total of five material parameters, namely the viscosity constant η_∞, the relaxation time τ and the three elastic parameters K_1, K_2 and K_3. In addition to K_1 and η_∞ also τ must be positive due to the definition $\tau^{-1} = 2\alpha_1 K_1$; to the entropy production only η_∞ and τ contribute:

$$R = 2\eta_\infty \left(A_{ij}\right)^2 + U_{ij}^0 \psi_{ij}/\tau. \qquad (167)$$

[1] L.D. Landau and E.M. Lifshitz E.M., *Fluid Mechanics,* (Butterworth, Oxford) 2002.
[2] I.M. Khalatnikov, *An Introduction to Superfluidity,* (Benjamin, New York) 1965.
[3] P.G. de Gennes and J. Prost, *The Physics of Liquid Crystals,* (Clarendon Press, Oxford) 1993.
[4] H. Pleiner and H.R. Brand H.R., *Pattern Formation in Liquid Crystals,* edited by A. Buka and L. Kramer, (Springer, New York) 1996, p.15.
[5] R.B. Bird, R.C. Armstrong, O. Hassager, *Dynamics of Polymeric Liquids, Vol.1* (John Wiley, New York, 1977).
[6] G. Strobl, *The Physics of Polymers* (Springer-Verlag Berlin Heidelberg, 1997).
[7] R.I. Tanner, *Engineering Rheology* (Oxford University Press, New York, 2000).
[8] R.G. Larson, *Constitutive Equations for Polymer Melts and Solutions,* (Butterworth) 1988.
[9] R.S. Graham, A.E. Likhtman, and T.C.B. McLeish, *J. Rheol.* **47**, 1171 (2003).
[10] M. Doi, S.F. Edwards, *The Theory of Polymer Dynamics* (Oxford University Press, New York, 1986).
[11] M.H. Wagner, M. Yamaguchi, and M. Takahashi, *J. Rheol.* **47**, 779 (2003).
[12] T.C.B. McLeish and R.G. Larson, *J. Rheol.* **42**, 81 (1998).
[13] H. Temmen, H. Pleiner, M. Liu, H.R. Brand, *Phys. Rev. Lett.* **84**, 3228 (2000).
[14] H. Temmen, Doktorarbeit, Universität Hannover (Shaker, Aachen, 1997).
[15] H. Temmen, H. Pleiner, M. Liu, and H.R. Brand, *Phys. Rev. Lett.* **86**, 745 (2001).
[16] H. Pleiner, M. Liu, and H.R. Brand, *Rheol. Acta* **39**, 560 (2000).
[17] H. Pleiner, M. Liu, and H.R. Brand, *Rheol. Acta* **43**, 502 (2004).
[18] Y.M. Jiang and M. Liu, *Granular Matter* **11**, 139 (2009).
[19] Y.M. Jiang and M. Liu, *Mechanics of Natural Solids*, edited by D. Kolymbas and G. Viggiani, (Springer, New York) 2009, p.27.
[20] G. Gudehus, Y.M. Jiang and M. Liu, *Granular Matter* **13**, 319 (2011).
[21] Y.M. Jiang and M. Liu, *Acta Mech.* **225**, 2363 (2014).
[22] Y.M. Jiang and M. Liu, *Eur. Phys. J. E* **38**, 15 (2015).
[23] H.B. Callen, *Thermodynamics and an introduction to thermostatics* (John Wiley & Sons, New York 1985).
[24] P.C. Martin, O. Parodi, P.S. Pershan, *Phys. Rev. A* **6**, 2401 (1972).
[25] S.R. De Groot, P. Mazur, *Grundlagen der Thermodynamik irreversibler Prozesse* (Bibliographisches Institut Mannheim, 1969).
[26] L.D. Landau. E.M. Lifschitz, *Elasticity Theory* (Akademie-Verlag Berlin, 1989).
[27] Using $\mathrm{Tr}(\mathbf{A}^n) = \sum_i A_i^n$, with A_i the eigenvalues, it is easy to show that $2\mathrm{Tr}(\mathbf{A}^4) - (\mathrm{Tr}(\mathbf{A}^2))^2 = 0$ for any traceless, symmetric tensor $\mathbf{A}$. For $\mathbf{U}$ this difference is at least proportional to $\mathrm{Tr}(\mathbf{U})$, and thus of higher order.
[28] In an Eulerian description, like the present one, $\dot\gamma$ is *not* the time derivative of the shear strain, as can be seen from Eq. (154). For historic reasons we keep the name "shear rate" and the symbol $\dot\gamma$. This remark applies analogously to the "elongational strain rate" $\dot\varepsilon$.
[29] L.R. Treloar, *J. Polym. Sci.: Polymer Symposium* **48**, 107 (1974).
[30] H.M. Laun, *Rheol. Acta* **17**, 1 (1978).
[31] J.D. Huppler, E. Ashare, L.A. Holmes, *Trans. Soc. Rheol.* **11**, 159 (1967).
[32] N. El Kissi, J.M. Piau, P. Attané, G. Turrel, *Rheol. Acta* **32**, 293 (1993).

[33] H. Kuchling, *Taschenbuch der Physik* (Fachbuchverlag Leipzig im Carl Hansen Verlag München Wien, 2004).
[34] J.D. Huppler, I.F. MacDonald, E. Ashare, T.W. Spriggs, R.B. Bird, L.A. Holmes, *Trans. Soc. Rheol.* **11**, 181 (1967).
[35] W.R. Leppard, E.B. Christiansen, AIChE J. **21**, 999 (1975).
[36] W.P. Cox, E.H. Merz, *J. Polym. Sci.* **28**, 619 (1958).
[37] E.B. Christiansen, W.R. Leppard, *Trans. Soc. Rheol.* **18**, 65 (1974).
[38] K. Weissenberg, *Nature* **159**, 310 (1947).
[39] D.D. Joseph, R.L. Fosdick, *Arch. Rational Mech. Anal.* **49**, 321 (1973).
[40] D.D. Joseph, G.S. Beavers, R.L. Fosdick, *Arch. Rational Mech. Anal.* **49**, 381 (1973).
[41] J. Serrin, *ZAMM* **39**, 295 (1959).
[42] R.I. Tanner, *Trans. Soc. Rheol.* **14**, 483 (1970).
[43] J. Meissner, *Rheol. Acta* **10**, 230 (1971).
[44] A.S. Lodge, *Elastic Liquids* (Academic Press, New York 1964).
[45] F.T. Trouton, *Proc. R. Soc.* **A77**, 426 (1906).
[46] J.M. Maerker, W.R. Schowalter, *Rheol. Acta* **13**, 627 (1974).